AD-A061 461 BERKELEY RESEARCH ASSOCIATES CA F/G 17/2.1
A GRADIENT DRIFT MICROSTRUCTURE MODEL.(U)
FEB 78 J B WORKMAN, S Y CHU DNA001-76-C-0136
UNCLASSIFIED BRA-78-171 DNA-4539T NL

1 OF 1
AD A061461

END
DATE FILMED
2 - 79
DDC

(12) LEVEL II

4539T

A GRADIENT DRIFT MICROSTRUCTURE MODEL

Berkeley Research Associates
Physical Dynamics, Inc.
P.O. Box 983
Berkeley, California 94701

February 1978

Topical Report for Period 1 November 1975—28 February 1978

CONTRACT No. DNA 001-76-C-0136

APPROVED FOR PUBLIC RELEASE;
DISTRIBUTION UNLIMITED.

THIS WORK SPONSORED BY THE DEFENSE NUCLEAR AGENCY
UNDER RDT&E RMSS CODE B322076464 S99QAXHC04106 H2590D.

Prepared for
Director
DEFENSE NUCLEAR AGENCY
Washington, D. C. 20305

Destroy this report when it is no longer needed. Do not return to sender.

(18) DNA, SRIF (19) 4539T, AD-E300 305

UNCLASSIFIED

SECURITY CLASSIFICATION OF THIS PAGE (When Data Entered)

REPORT DOCUMENTATION PAGE	READ INSTRUCTIONS BEFORE COMPLETING FORM
1. REPORT NUMBER: DNA 4539T	2. GOVT ACCESSION NO. / 3. RECIPIENT'S CATALOG NUMBER
(6) 4. TITLE (and Subtitle): A GRADIENT DRIFT MICROSTRUCTURE MODEL.	(9) 5. TYPE OF REPORT & PERIOD COVERED: Topical Report. 1 Nov 75—28 Feb 78.
	(14) 6. PERFORMING ORG. REPORT NUMBER: BRA-78-171
(10) 7. AUTHOR(s): J. B. Workman, S. Y. F. Chu	(15) 8. CONTRACT OR GRANT NUMBER(s): DNA 001-76-C-0136
9. PERFORMING ORGANIZATION NAME AND ADDRESS: Berkeley Research Associates, Physical Dynamics, Inc., P.O. Box 983, Berkeley, California 94701	10. PROGRAM ELEMENT, PROJECT, TASK AREA & WORK UNIT NUMBERS: (16) Subtask S99QAXHC041-06
11. CONTROLLING OFFICE NAME AND ADDRESS: Director, Defense Nuclear Agency, Washington, D.C. 20305	(11) 12. REPORT DATE: Feb 78 / 13. NUMBER OF PAGES: 82
14. MONITORING AGENCY NAME & ADDRESS (if different from Controlling Office) (12) 81p.	15. SECURITY CLASS (of this report): UNCLASSIFIED
	15a. DECLASSIFICATION/DOWNGRADING SCHEDULE
16. DISTRIBUTION STATEMENT (of this Report): Approved for public release; distribution unlimited.	(17) C041
17. DISTRIBUTION STATEMENT (of the abstract entered in Block 20, if different from Report)	
18. SUPPLEMENTARY NOTES: This work sponsored by the Defense Nuclear Agency under RDT&E RMSS Code B322076464 S99QAXHC04106 H2590D.	
19. KEY WORDS (Continue on reverse side if necessary and identify by block number): Nuclear Effects, Striations, Plasma Microstructure, Gradient Drift	
20. ABSTRACT (Continue on reverse side if necessary and identify by block number): An approximate theoretical and numerical model for gradient drift microstructure has been developed. While it is believed to be completely consistent with all current theoretical understanding of the physics, the model is quite flexible and adjustable so as to provide agreement with the experimental data base. Capable of spanning many orders of magnitude in scale size, the model provides the mechanics of cascade and ultimate diffusion required for late time studies.	

DD FORM 1 JAN 73 1473 EDITION OF 1 NOV 65 IS OBSOLETE

78 07 14 048

UNCLASSIFIED

SECURITY CLASSIFICATION OF THIS PAGE (When Data Entered)

393 694

PREFACE

The authors wish to acknowledge the invaluable assistance of C. Prettie in the theory and development of this model.

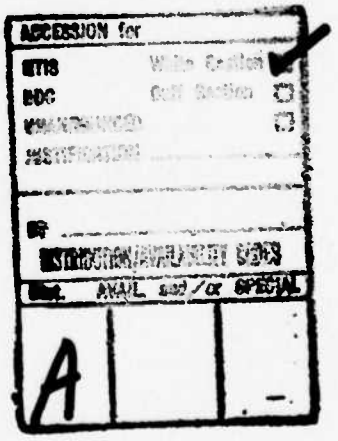

CONTENTS

LIST OF ILLUSTRATIONS

I. INTRODUCTION

The important role of gradient drift microstructure in the analysis of UHF radio transmission in the high-altitude nuclear environment has been recognized for some years. The use of specific microstructure realizations to study propagation effects is rather commonplace. The modelling of microstructure using the principles of gradient drift physics has not previously been done, however. It may appear paradoxical that the scientific community has taken so long to tackle this issue in view of the considerable research on striation physics in the last several years. The explanation is essentially a question of priorities and the perceived needs of the users. For applications which emphasize the early time evolution of plasma structure, the propagationists have been satisfied with the convenient type of modelling devised by Chesnut which is a data fit to experimental results. Recently, this type of approach has been extended by Rino and Sachs. Conversely, the phenomenologists have been concentrating their energy on understanding and codifying the basic neutral and plasma background parameters which drive the fine scale development.

Using a single, simple variable such as $\delta n/n$, it is possible to link the Chesnut type of modelling to background calculations and carry out various types of systems studies. There is, of course, the inherent assumption that the background physics is not only independent of the model details, but, furthermore, even of the existence of microstructure.

The recent interest in conducting studies of plasma development over very extended periods of time has, however, placed a great strain on the credibility of current

computational techniques. In the first place, there is the problem of using data fit models in regimes that are not even remotely similar to those corresponding to the regimes in which the data was gathered. Users are no longer able to argue that, even if the physics is absent, the modelling is a real representation of experimental facts. In the second place, the phenomenologists are recognizing that interactive effects with the background, such as striation convection and striation decay, cannot be investigated without constructing some sort of microstructure model that relates to the real plasma physics.

Viewed as a general proposition, the construction of a first principles microstructure model is one of the most challenging tasks faced by the nuclear effects community. The phenomena, like ordinary fluid turbulence, does not permit direct numerical simulation. The range of relevant scale sizes is enormous, covering perhaps four orders of magnitude in at least a two-dimensional space. Even if one could generate actual full-scale plasma realizations, the propagationists would find this an unmanageable data and calculational morass. Particularly from a systems analysis standpoint, the direct manipulation of total plasma density information is unthinkable.

Fortunately, it is generally recognized that a power spectrum of the plasma density fluctuations, fitted to some simple analytic form, is both an adequate description and represents the maximum usable information in most applications. Recent work by Wittwer has been invaluable in demonstrating this important conclusion. Insomuch as specific realization models are employed, they are not claimed to be point-by-point exact simulations of particular real world plasma distributions. They are, in fact, models

which claim statistical equivalence to actual distributions. This equivalence is established by fitting both data and model to a common power spectra in the usual case. Note that an autocorrelation of the density fluctuations is identical to the power spectrum. Likewise, statistical correlations of the electromagnetic variables are effectively the same thing, but require an unfolding operation.

If we only wished to satisfy the propagationists, we would build a power spectral model. Fortunately, this is exactly the tool that the physics will also require. It is, in fact, we believe, the only item that deterministic physics can provide with certainty. All other quantities will prove to be statistical correlations of random variables.

There are two key features to the modelling that will be presented in subsequent sections. First, it will be carried out in Fourier space. Second, it will combine Fourier modes into a lumped parameter system. This will be similar to the lumping of molecular collision processes in defining chemical kinetics. We believe that the end result represents a significant breakthrough in understanding and describing plasma microstructure.

II. THE CHARACTER OF MICROSTRUCTURE

While the general deterministic description of plasma microstructure is an unresolvable problem, there are a series of assumptions which will permit an approximate solution. The plasma evolution begins in a scenario with only a limited range of large-scale sizes. Experience and intuition tell us that it is only this range which is peculiar or specific to a given example. The vast majority of smaller sizes possess general or statistical properties which are not tied to specific scenarios. Obviously, if this were not the case, there would be no point to any experimental or numerical simulation short of a real detonation. As an observational fact, we note that the overall appearance of gradient drift microstructure is similar, regardless of the original source.

We assume that the general properties of the structure are calculable using suitable, approximate physical models. Likewise, we assume that these properties are adequate for propagation studies. The nature of the general representation is a power spectrum of the plasma perturbations (from the mean).

The plasma power spectrum possesses a number of useful features which allow the simplicity necessary for actually constructing a working model. The summation or integration of power spectral amplitudes is essentially a conserved quantity. This principle underlies model construction. Information concerning "plasma phase" is lost in the description. However, this is not necessary for either the hydrodynamics or propagation in the "many striation" limit. Transfer of power between regimes in Fourier spece is governed by gradient drift processes.

The analytic format of the transfer rates is derivable from theoretical studies.

Of considerable importance is the fact that rate constants and parameters have a generality analogous to chemistry in molecular kinetics. Thus, data can be deduced from a variety of external sources including field experiments.

The distribution of power within spectral regimes is assumed to obey certain simple monotonic functions. This permits a lumped parameter representation of each regime. From experience and for model convenience, we have chosen to divide the spectrum into four regimes. The first is the macroscopic or exact code regime. It comprises the largest scales which vary in specific patterns peculiar to the particular scenario. This regime is <u>not</u> modelled, but does provide the necessary inputs and boundary parameters to drive the power spectrum model.

To clarify the discussion of scale size range, let us consider a ray path through a typical battle space grid as in Figure 1. The disturbed (or potentially disturbed) portion of the path is the segment, L. In principle, as either a propagationist or a phenomenologist, we would like a description of the plasma density distribution along and in the vicinity of this line. For the largest sizes, we would compute the plasma properties using an "exact code". These macroscopic sizes would depend ultimately on the particular scenario and we would desire a completely deterministic computation. Using the terminology of "Fourier space", we would require information on the "plasma phase". For purposes of discussion, however, let us conceive of creating a plasma power spectrum from the data such a code would provide.

PROPOGATION IN THE BATTLE SPACE GRID

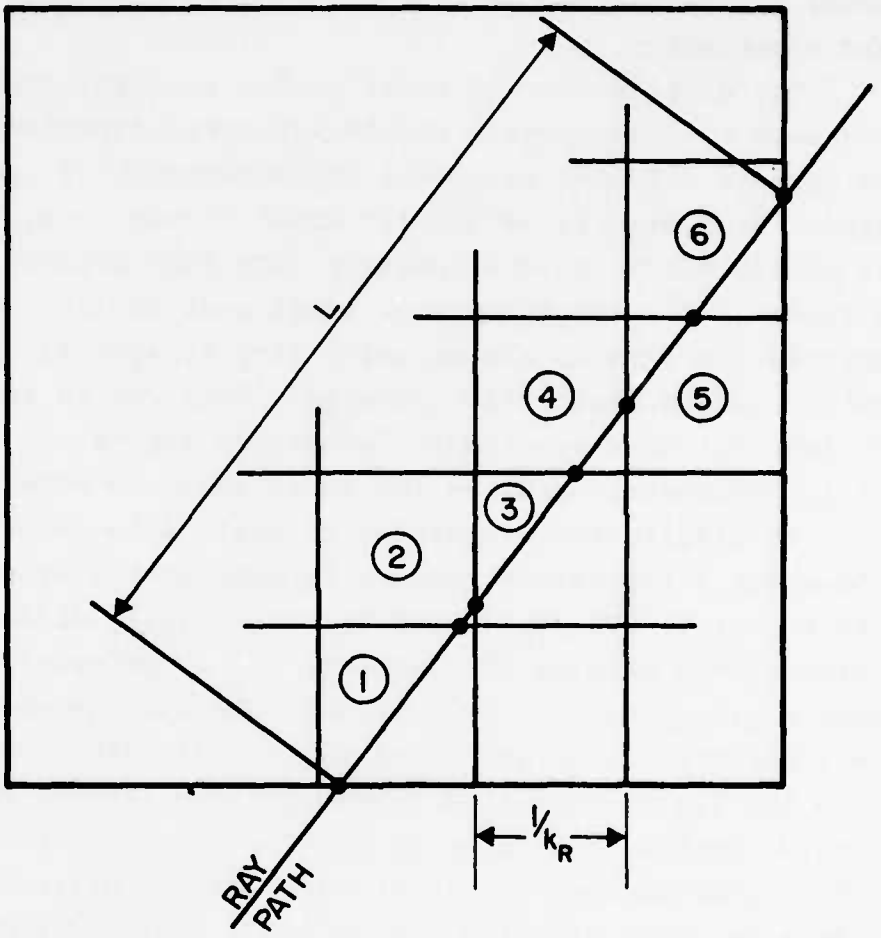

Figure 1. Propagation in the battle space grid.

In Figure 2, we show a power spectral plot that might result from the Fourier analysis of the ray path in Figure 1. The "exact code" could generate a nonzero spectrum only out to some wavenumber, k_R, which corresponds to the minimum grid dimension in the macroscopic code. The spectrum would be generated by analysis of the complete ray path segment and provide a result as indicated by the curve labeled "all boxes". The symbols, k_o and f_o^2, which characterize the power spectral properties are shown for future reference and will not be discussed in detail here.

In practice, the basic grid dimension, as characterized by k_R, is usually no less than 50-100 km. Thus, the plasma data available from the plasma grid itself is hardly in the "striation regime".

The modelling of microstructure which forms the topic of the present paper is concerned with filling in the details for each of the small boxes shown in Figure 1. In applications, the model will be used to describe the particular behavior of plasma in many, many boxes simultaneously. Turning again to Figure 2, the schematic attempts to show the fact that each box will have its own local power spectrum. The microstructure model for each volume will generate data only for the wavenumber range greater than k_R. Of the four Fourier space regimes mentioned earlier, three of them are, obviously, the components of the microstructure model. The curve labeled "Box 1" in Figure 2, is a good example of a spectrum which contains power in each of these three lumped parameter idealizations. In the following discussion, we will outline the functional behavior that we assume for each of these regimes.

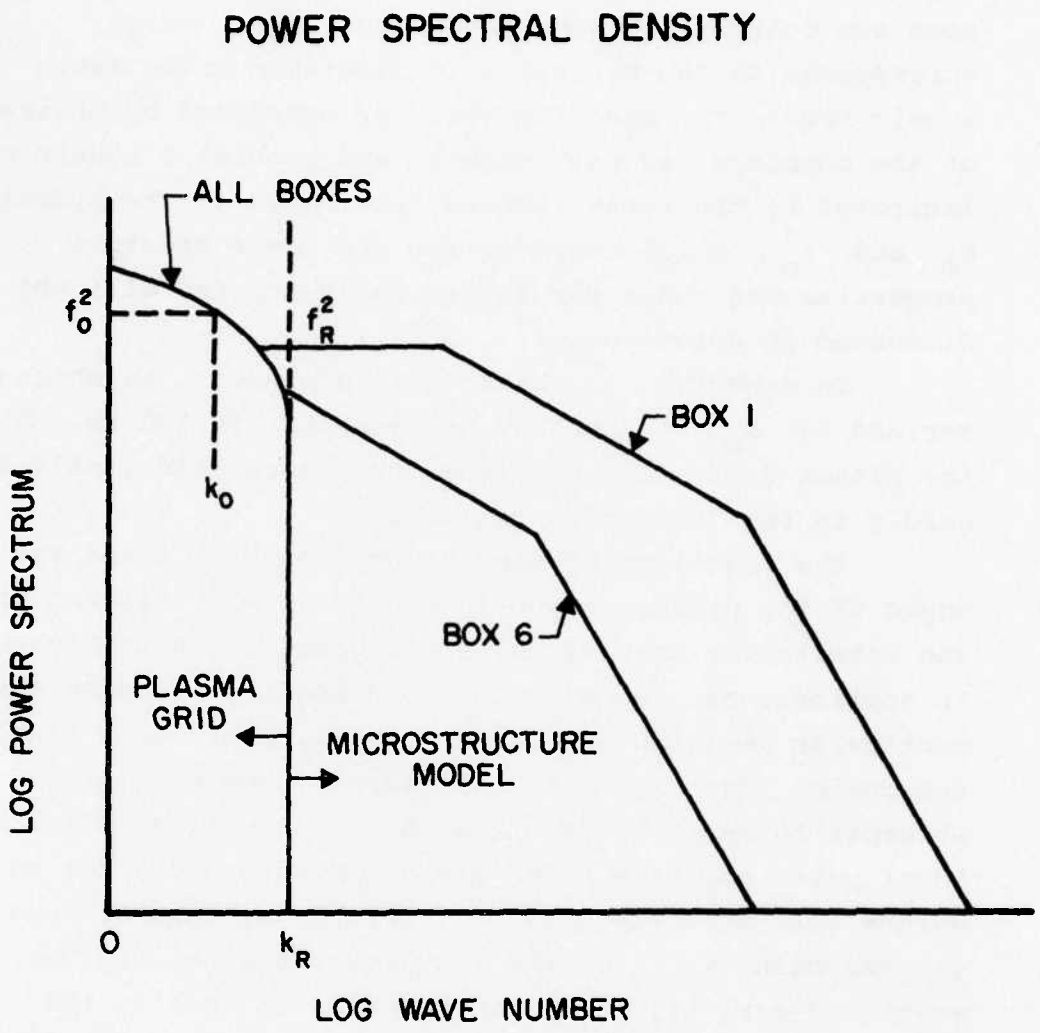

Figure 2. Power spectral density.

A connector or "reservoir" regime is defined as a convenient artifice to connect the deterministic macroscopic scales to the statistical modelling of the true microscopic regimes. Of use primarily in transient processes, it is assumed (somewhat arbitrarily) to have a flat noise-like spectrum (k^0).

The fully developed or "cascade" regime is assumed to dominate whenever the gradient drift process can operate without strong transient boundary conditions. It is the classic or fully developed spectrum which varies as $1/k^2$. Observed both in experimental data and in numerical simulation results, we believe the $1/k^2$ dependence is the consequence of Fourier transforming "sharp edges". The convection of density enhancements relative to density rarefactions is the essence of the gradient drift mechanism. The process always results in a high density piece of plasma flowing away from its neighbors, exposing itself to a low density background, and creating a sharp gradient (hence the name of instability). Because the fluid is essentially incompressible, very sharp gradients can remain for extended periods of time. The only process that limits the growth of gradients is electron diffusion, which is significant only at very small scale lengths (very large wavenumbers). In the wavenumber range where diffusion is important, it will "eat up" or absorb the plasma power leading to a much steeper decline in power versus wavenumber.

The sink or "diffusion" regime exists for the very smallest sizes which are subject to significant crossfield diffusion. It has a steep dependence and is presently modelled with a $1/k^6$ variation based on analytic studies of Kilb.

Figure 3 is a schematic diagram which pictorially displays the nature of the various power spectral regimes. The function of the microstructure model is to compute the Fourier space extent and the total power for each characteristic regime.

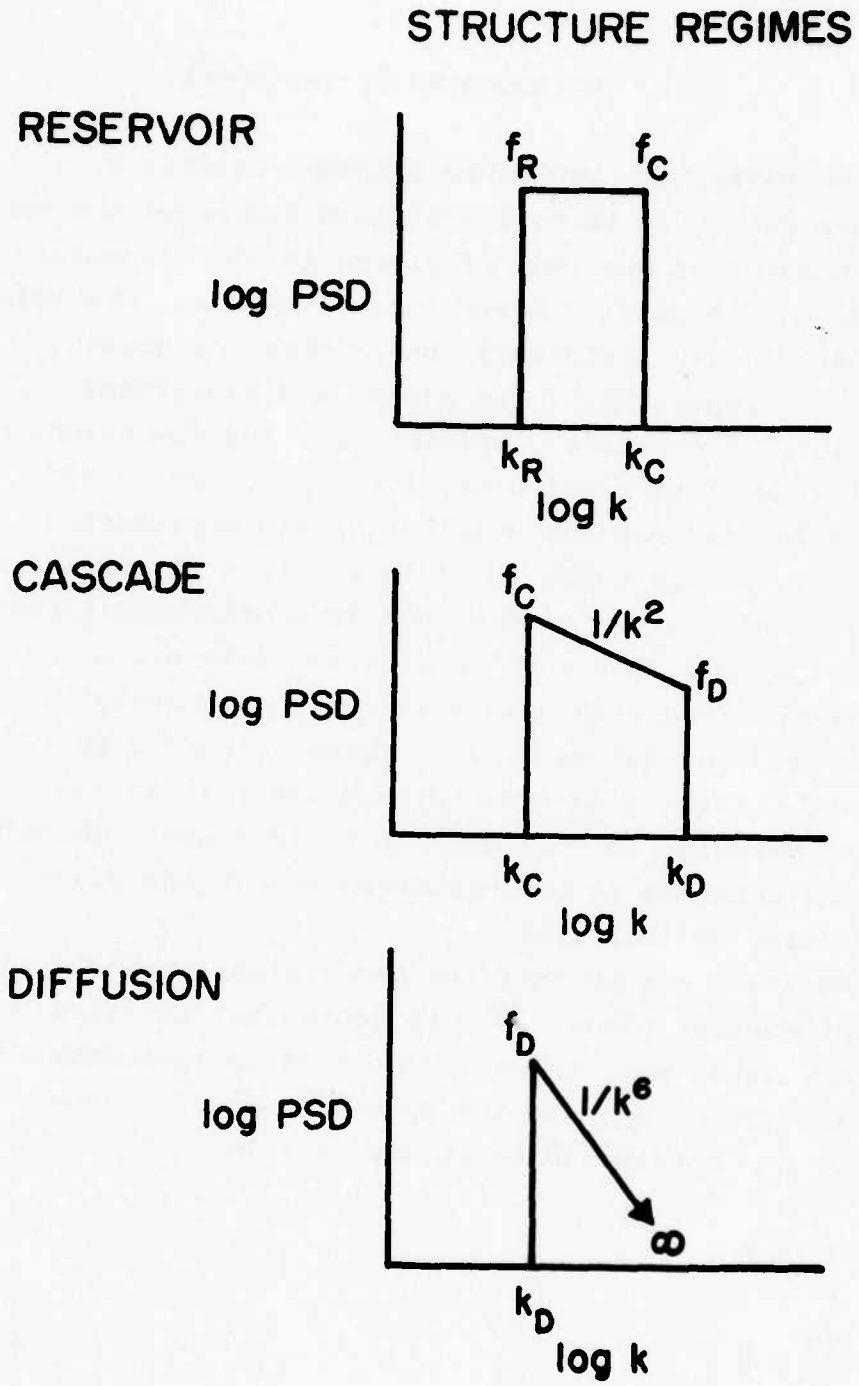

Figure 3. Structure regimes.

III. DEVELOPMENT OF THE MODEL

A. INCOMPRESSIBILITY AND POWER SPECTRAL SUMMATION

Our objective is to investigate and model the gradient drift mechanics of a volume of plasma in the ionosphere according to the usual F-layer approximations. The volume to be modelled is sufficinetly small that the gross, macroscopic properties of the plasma and background can be assumed locally constant. Nonetheless, the dimensions of this volume will be treated as, typically, orders of magnitude larger than the smallest possible striation dimensions. We can conceive of this volume as corresponding in size to the minimum grid volume in a macroscopic plasma hydrodynamic code, although we will not make a one-to-one correspondence with such a volume in the analytic development. The volume will be taken as sufficiently local that there is no structure of interest in the direction parallel to the magnetic field lines. Therefore, all of the dynamics to be considered are in the plane perpendicular to this field.

We shall assume that the gross plasma velocity in the perpendicular plane, $\vec{U}$, is equivalent to $(\vec{E}\times\vec{B})/B^2$. Therefore, as is well known in the F-layer approximation, $\vec{U}$ is divergence free and the dynamics of the plasma density, n, correspond to incompressible flow.

$$\nabla_{\perp}\cdot\vec{U} = 0 \qquad (1)$$

and

$$\frac{Dn}{Dt} = 0 \qquad (2)$$

As with the density itself, any function of density alone is, likewise, a preserved Lagrangian quantity. Specifically,

the square of plasma density, n^2, is such a quantity.

$$\frac{Dn^2}{Dt} = 0 \tag{3}$$

The divergence free flow (or incompressible flow) is equivalent to a statement that an area, A, in the plane defined by marker particles in the plasma is a preserved quantity. Therefore, spatial averages of any function of density are, likewise, preserved in a Lagrangian sense. In particular, the average of the density, $\overline{n}$

$$\overline{n} = \frac{1}{A}\iint n \; d \; A \tag{4}$$

and the average of the density squared, $\overline{n^2}$

$$\overline{n^2} = \frac{1}{A}\iint n^2 \; d \; A$$

are preserved

$$\frac{D\overline{n}}{Dt} = 0 \tag{5}$$

and

$$\frac{D\overline{n^2}}{Dt} = 0 \tag{6}$$

All of the statements above come directly from the fact that the gross plasma motion is assumed to be given by $(\vec{E}\times\vec{B})/B^2$. The other major assumption that will be employed in the development, at this point, is a statement concerning the plasma power spectrum.

It is customary for both propagation and phenomenological purposes to assume that the one-dimensional plasma

power spectrum in the plane perpendicular to the magnetic field is locally independent of direction. There is no explicit mathematical proof or approximation based on the general plasma equations to substantiate this statement. On the other hand, there is also no theoretical reason to believe that it is an incorrect concept when applied to well-developed plasma structure. Intuitively, it is an attractive hypothesis which draws on analogies to conventional fluid turbulence and molecular chaos in kinetic theory. From a purely practical standpoint, it is undoubtedly the only avenue available to modellers of gradient drift mechanics. Unless clearly contradicted by new theoretical or experimental developments, it is likely to be with us for a long time. From the standpoint of the present paper, there would, in fact, be difficulty in acceptance or application of the work if this feature were not built into the model. It should be noted in passing that an anisotropic spectrum could be employed if the general theory were developed and the users were willing to apply it.

Conceptually, a one-dimensional plasma power spectrum is created along a trace in any direction, x, by Fourier transforming the distribution of plasma density. The complex spectral amplitude, $\hat{g}$, is given by

$$\hat{g}(k) = \int_{-\infty}^{\infty} n(x)\ e^{ikx}\ dx \qquad (7)$$

where k is the wavenumber. The power spectral distribution (PSD) is given by

$$PSD(k) = \hat{g}\ \hat{g}^* \qquad (8)$$

where $\hat{g}^*$ is the complex conjugate and the PSD is, of course, a real positive number distribution.

In actual use, either in analyzing data or in performing numerical simulations, it is convenient to work with finite Fourier representations created over some span in x of extent $2L$. The plasma density over this span is given by a summation as

$$n(x) = \sum_j \hat{f}_j \, e^{i\theta_j} \, e^{ik_j x} \tag{9}$$

where $\hat{f}_j$ is the real polar modulus of a complex amplitude and θ_j is the "plasma phase". A "discrete PSD" can be created from (9) of the form

$$PSD(k_j) = \hat{f}_j^2 \tag{10}$$

It should, of course, be noted that (8) and (10) are not identical and, in fact, are not the same dimensionally. They can, however, be simply related through the span length, $2L$.

$$PSD(k) = (4L^2) \; PSD(k_j) \tag{11}$$

where the k_j are intepreted as points on a continuous curve for making the correspondence. There are, in addition, a variety of other ways of normalizing or scaling the PSD depending on the application, but the relationship is similar in form to (11). Our objective in the present discussion is to establish a connection between the PSD parameters and the conserved density parameters. For convenience in this task we will ultimately find it desirable to introduce a third form of PSD representation, which will be developed in the material below.

Using the form (9), let us construct a Fourier expression for the plasma density squared, n^2, over a span in x of extent $2L$.

$$n^2(x) = \sum_{\ell} \sum_{j} \hat{f}_\ell \, \hat{f}_j \, e^{i(\theta_\ell + \theta_j)} \, e^{i(k_\ell + k_j)x} \tag{12}$$

Now, let us find the average value of the quantity over the span as follows

$$\overline{n^2} = \frac{\int_{-L}^{L} n^2(x) \, dx}{2L} \tag{13}$$

Before performing the integration, we should recall an important property of the orthogonal Fourier terms, namely,

$$\int_{-L}^{L} e^{i(k_\ell + k_j)x} \, dx = 0 \quad ; \quad \text{for} \quad k_\ell + k_j \neq 0 \tag{14}$$

Thus, the only terms which will contribute are the ones where $k_\ell = k_{-j}$. Therefore, the integration of (12) in (13) results in the simpler expression

$$\overline{n^2} = \sum_{j} \hat{f}_j \, \hat{f}_{-j} \, e^{i(\theta_j + \theta_{-j})} \tag{15}$$

Because n is a <u>real</u> variable, the Fourier coefficients also possess another well-known property, namely,

$$\hat{f}_j = \hat{f}_{-j}$$

and

$$\theta_j = -\theta_{-j} \tag{16}$$

Ultimately, then, we obtain the very simple result that

$$\overline{n^2} = \sum_j \hat{f}_j^2 \tag{17}$$

Equation (17) tells us that the average density square in the plasma, along a span in x of extent $2L$, is equal to the summation of the discrete PSD terms along the same span. It is at this point, obviously, where we will employ the assumption that the PSD is independent of direction. We say that we could have placed the span $2L$ in any direction, at any location in the area, A, and obtained the same result for the average square of the plasma density. Therefore, the result given by (17) must be the true average density for the entire area, A, and does not apply just to a specific, arbitrary, one-dimensional span. Using (6), we then obtain the powerful conservation principle that

$$\frac{D}{Dt}\left[\sum_j \hat{f}_j^2\right] = 0 \tag{18}$$

It is convenient to re-express in a different form for actual use in model construction or numerical application. First, it will simplify expressions at a later point if $\hat{f}_j$ is normalized by the local average density, $\overline{n}$. Because $\overline{n}$ is preserved as shown in (5), it can be multiplied out of the expression

$$f_j \equiv \frac{\hat{f}_j}{\overline{n}} \tag{19}$$

and

$$\frac{D}{Dt}\left[\sum_j f_j^2\right] = 0 \tag{20}$$

Second, it will be easier to manipulate (20) if we can approximate it by an integral expression. Defining the wavenumber interval in the discrete transform as

$$k_{j+1} - k_j = \Delta k = \frac{\pi}{L} \tag{21}$$

we can convert f_j to a continuous function f as follows

$$\sum_j f_j^2 = \int_0^\infty \frac{L}{\pi} f^2(k)\, dk \tag{22}$$

For simplicity, let us define a new symbol F as follows

$$F \equiv \int_0^\infty f^2(k)\, dk \tag{23}$$

Thence

$$\sum_j f_j^2 = \frac{L}{\pi} F \tag{24}$$

Finally, we obtain the simple desired expression

$$\frac{DF}{Dt} = 0 \tag{25}$$

It will be convenient to refer to F or components of F as the "power spectral summation". Note, however, that care must be used in actual numerical calculation. A characteristic, fixed scale length, L, is always associated with any given problem. It is usually desirable

to fix this quantity at some convenient reference level throughout the temporal and spatial evolution of a scenario. In a numerical simulation which employs a macroscopic hydrodynamic plasma code, this dimension would be of the order of the minimum grid dimension (although it need not be exactly equivalent). In interpreting or manipulating data, this dimension might be chosen as a span corresponding to a characteristic dimension in the disturbed plasma.

We will typically display a "power spectral density result" by plotting f^2 as a function of k. The actual numbers will, of course, depend on the value of L that is characteristic of that particular calculation. Note that the summation, F, must always be multiplied by L to obtain a dimensionless value that is directly related to the local average square of the dimensionless density.

Using the expressions developed in this section, we can readily convert any specific PSD or summation, F, to any arbitrary scale length expresssion by simple multiplication, thus

$$f_A^2 = f_B^2 \left(\frac{L_A^2}{L_B^2} \right) \tag{26}$$

and

$$F_A = F_B \left(\frac{L_B}{L_A} \right) \tag{27}$$

Note, however, that in a real problem we can never avoid the scale length specification, L. Letting L go to infinity, for example, and thus using a "true PSD", $g^2(k)$, or a "true summation", G, is mathematically clean, but

will always be ill-defined and indeterminate in an actual computation.

B. GRADIENT DRIFT RATES

As discussed in an earlier section, the microstructure model is constructed by lumping plasma spectral power into several distinct groups. The groups are assumed to have distinctive statistical features and are organized according to their position in Fourier space. Specifically, let us repeat Equation (23) which defines the total spectral summation

$$F \equiv \int_0^\infty f^2 \, dk \tag{23}$$

Now let us break the integral into four distinct parts

$$\begin{aligned}
F_O &= \int_0^{k_R} f^2 \, dk \quad \text{macroscale} \quad 0 < k < k_R \\
F_R &= \int_{k_R}^{k_C} f^2 \, dk \quad \text{reservoir} \quad k_R < k < k_C \\
F_C &= \int_{k_C}^{k_D} f^2 \, dk \quad \text{cascade} \quad k_C < k < k_D \\
F_D &= \int_{k_D}^{\infty} f^2 \, dk \quad \text{diffusion} \quad k_D < k < \infty
\end{aligned} \tag{28}$$

where $F = F_O + F_R + F_C + F_D$.

From Equation (25), we establish that F is a preserved Lagrangian quantity in the absence of collisional/diffusion effects. Crossfield diffusion is generally thought of as negligible in the F-layer ionosphere, when the usual macroscopic scale sizes are considered. On the other hand, the present microstructure modelling is arranged to extend down to very small sizes and, by definition, diffusion effects must be considered in the largest k group. Diffusion, in fact, is a necessary ingredient in constructing a complete life cycle history for plasma structure. There is no other hydrodynamic mechanism for ultimately removing striations. The construction of an appropriate correction term for the conservation equation will be the subject of the next subsection. For the moment, we will merely indicate, in words, the presence of such a term.

Qualified by the statement above on diffusion, we can express the basic conservation equation for the total spectral summation

$$\frac{dF_O}{dt} + \frac{dF_R}{dt} + \frac{dF_C}{dt} + \frac{dF_D}{dt} = -\text{diffusion} \qquad (29)$$

The objective of the present subsection is to construct rates which define the transfer of power between the various spectral groups. Specifically, we wish to construct a matrix of rate expressions of the form

$$\frac{dF_O}{dt} = -R_{OR} - R_{OC} - R_{OD}$$

$$\frac{dF_R}{dt} = R_{OR} - R_{RC} - R_{RD}$$

$$\frac{dF_C}{dt} = R_{OC} + R_{RC} - R_{CD}$$

$$\frac{dF_D}{dt} = R_{OD} + R_{RD} + R_{CD} - \text{diffusion} \qquad (30)$$

In transferring power from one wavenumber regime to another, we use a symbol, R_{mn}, for the rate, where m corresponds to the large size regime from which power is removed and n corresponds to the smaller size regime to which power is added.

Simple gradient drift theory has demonstrated that mode amplitudes in regime n grow from gradients in regime m with the following rate.

$$\frac{d\, f_n}{dt} = -(\Delta U) \left(\frac{\nabla n}{n}\right)_m f_n \qquad (31)$$

where ΔU is the ion-neutral slip velocity and f_n is the real polar amplitude of a perturbation seed of form $f_n\, e^{ik_n x}$.

Consider a large scale plasma structure over the span, $2L$, which is describable by a finite Fourier series of the form

$$n_m(x) = \bar{n}_m \left(1 + \sum_{j=0}^{m} f_j\, e^{i\theta_j}\, e^{ik_j x}\right) \qquad (32)$$

The growth scale given in (31) can then be expressed as

$$\frac{1}{d} = -\left(\frac{\nabla n}{n}\right)_m = -\frac{\sum^{m} ik_j\, f_j\, e^{i\theta_j}\, e^{ik_j x}}{1 + \sum^{m} f_j\, e^{i\theta_j}\, e^{ik_j x}} \qquad (33)$$

We cannot, of course, consider the general nonlinear evolution of growth in Fourier space any more easily than in physical space. Thus, we will consider a plasma wherein the structured plasma distribution represents only a small perturbation from the mean. This assumption permits us to drop the nonlinear term in the denominator of (33)

$$\frac{1}{d} \approx - \sum^{m} ik_j f_j e^{i\theta_j} e^{ik_j x} \tag{34}$$

Over the span, $2L$, which contains the large wavelength plasma structure with growth scale distribution, $d(x)$, given by (34), let us insert a single small wavelength mode of initial uniform amplitude, f_{n_o}. Locally, as a function of x, the familiar gradient drift growth expression (31) tells us that the amplitude will grow as

$$f_n(x,t) = f_{n_o} e^{\frac{\Delta U}{d(x)} t} \tag{35}$$

As the use of the procedures developed here is for ultimate employment in a finite difference, time stepping numerical code, we need only follow the growth for "short times" with analytical expressions such as (35). Our objective is, thus, to linearize the results of (35) in a convenient finite different format. We shall expand the exponential in (35) as a power series of time. We will discover that we must keep terms to second order, however, to obtain a net positive average growth.

$$f_n(x,t) \approx f_{n_o} \left[1 + \left(\frac{\Delta U}{d}\right) t + \frac{1}{2} \left(\frac{\Delta U}{d}\right)^2 t^2 \right] \tag{36}$$

The average net growth of f_n across the span is given by

$$\overline{f_n(t)} = f_{n_o}\left[1 + (\Delta U)\,t\left(\overline{\frac{1}{d}}\right) + \frac{1}{2}(\Delta U)^2 t^2\left(\overline{\frac{1}{d^2}}\right)\right] \tag{37}$$

where

$$\left(\overline{\frac{1}{d}}\right) = \frac{1}{2L}\int_{-L}^{L} - \sum^{m} ik_j f_j e^{i\theta_j} e^{ik_j x}\,dx \tag{38}$$

and

$$\left(\overline{\frac{1}{d^2}}\right) = \frac{1}{2L}\int_{-L}^{L}\sum_{j}^{m}\sum_{\ell}^{m} k_j k_\ell f_j f_\ell e^{i(\theta_\ell+\theta_j)} e^{i(k_j+k_\ell)x}\,dx \tag{39}$$

We should note that the character of these integrations is identical to that of the last subsection and lead to analogous results, namely,

$$\left(\overline{\frac{1}{d}}\right) = 0 \tag{40}$$

and

$$\left(\overline{\frac{1}{d^2}}\right) = \sum^{m} k_j^2 f_j^2 \tag{41}$$

We now rewrite (37) as a differential expression and drop some of the complicating notation, recognizing that, henceforth, all quantities refer to average values across the span

$$\frac{df_n}{dt} = \gamma^2 f_n t \tag{42}$$

where the growth rate, γ, is

$$\gamma = (\Delta U)\sqrt{\sum^{m} k_j^2 f_j^2} \tag{43}$$

Note that Equation (42) remains nonlinear in time and will not prove satisfactory for use in constructing a viable rate expression. We, thus, desire to linearize (42). To do this, we must pick some characteristic time and the only obvious choice, of course, is the inverse of the growth rate itself, $1/\gamma$. There results our final, linear expression for gradient drift growth in Fourier format

$$\dot{f}_n = \gamma f_n \tag{44}$$

The summation shown in (43) is not a convenient quantity to work with. Let us, first, cast it in integral format similar to (22) and (23) by defining a new parameter, H

$$H_m \equiv \int^{m} k^2 f^2(k)\, dk = \frac{\pi}{L} \sum^{m} k_j^2 f_j^2 \tag{45}$$

Second, let us relate this parameter directly to the definition of F in (23) by an additional parameter, $\bar{k}$

$$(\bar{k}_m)^2 \equiv \frac{H_m}{F_m} \tag{46}$$

Utilizing $\bar{k}$, we can express (44) in terms of quantities defined in the last subsection

$$\frac{df_n}{dt} = \Delta U\, \bar{k}_m \sqrt{\frac{L}{\pi} F_m}\; f_n \tag{47}$$

Note that (47) is equivalent to

$$\frac{1}{2}\frac{d\, f_n^2}{dt} = \Delta U\, \bar{k}_m \sqrt{\frac{L}{\pi} F_m}\; f_n^2 \qquad (48)$$

Again using the definition of (23), we recall that the integration of f_n^2 acrosss its extent in Fourier space is given by

$$F_n = \int^n f_n^2\, dk \qquad (49)$$

We can thus integrate (48) in Fourier space and use (49) to simplify the result

$$\frac{1}{2}\frac{d\, F_n}{dt} = (\Delta U)\, \bar{k}_m \sqrt{\frac{L}{\pi} F_m}\; F_n \qquad (50)$$

Equation (50) respresents the rate expression that we sought in constructing the general kinetic format of (30). Thus, we can write

$$R_{mn_\alpha} = 2(\Delta U)\, \bar{k}_m \sqrt{\frac{L}{\pi} F_m}\; F_n \qquad (51)$$

The subscript α has been appended to R_{mn} to indicate that (51) refers to "seed growth". That is, it represents that type of gradient drift power transfer, from regime m to regime n, which occurs when regime n already contains a "seed"--indicated in this instance by the presence of F_n. Note that, if there were no structure in regime n ($F_n = 0$), this class of power transfer would not be operative. We, thus, know that there must be other mechanisms for transferring power in addition to the specific process that we have modelled here. Both from experiment and from numerical simulation, we observe

that power can flow from regime m to regime n in the absence of any initial power in regime n. We do observe, however, that the flow of power can be greatly enhanced once a "seed" has been established. We would conclude that, while a rate of the form R_{mn_α} may be dominant, it is not the only rate that we will need to model in a complete representation.

Seed growth is the only gradient drift transfer process that has proven amenable to any extensive analytic or theoretical development. Thus, by comparison, it has been relatively easy and straightforward to model. Nonetheless, at this point, we must proceed to formulate the other type of mechanism, commonly called "bifurcation", that is thought to be important.

To understand bifurcation, it is useful to return to the basic plasma convection equation. Both in observing numerical simulations and in the theoretical studies that do exist, it appears that the nonlinear mechanics represented by this equation are primarily responsible for the power transfer from large to small sizes.

Consider the convection equation in the following Eulerian form

$$\frac{\partial n}{\partial t} = - \left(\frac{\partial n}{\partial \vec{x}}\right) \cdot \left(\frac{\partial \psi}{\partial \vec{x}}\right) \tag{52}$$

where ψ is the plasma velocity stream function

$$\frac{\partial \psi}{\partial \vec{x}} = \vec{U} \tag{53}$$

Let us express both the density, n, and stream function, ψ, in Fourier form

$$n = \sum_j a_j \, e^{ik_j \vec{x}} \tag{54}$$

$$\psi = \sum_\ell b_\ell \, e^{ik_\ell \vec{x}} \tag{55}$$

We will omit some of the fine points of notation in the discussion for clarity. We are merely interested in illustrating the qualitative behavior and are not conducting a mathematical proof. Note that a_j represents the complex density modal amplitudes, while b_ℓ represents the similar quantities for the stream function. Substituting (54) and (55) into (52) yields

$$\sum_j \dot{a}_j \, e^{ik_j \vec{x}} = \left(\sum_j \vec{k}_j \, a_j \, e^{ik_j \vec{x}} \right) \cdot \left(\sum_\ell k_\ell \, b_\ell \, e^{ik_\ell \vec{x}} \right) \tag{56}$$

The nonlinear operation is the convolution of the RHS of (56) into a new single summation

$$\left(\sum_j \vec{k}_j \, \dot{a}_j \, e^{ik_j \vec{x}} \right) \cdot \left(\sum_\ell \vec{k}_\ell \, b_\ell \, e^{ik_\ell \vec{x}} \right) = \sum_m c_m \, e^{ik_m \vec{x}} \tag{57}$$

such that (56) becomes

$$\sum_j \dot{a}_j \, e^{ik_j \vec{x}} = \sum_m c_m \, e^{ik_m \vec{x}} \tag{58}$$

or

$$\dot{a}_j \, e^{ik_j \vec{x}} = c_m \, e^{ik_m \vec{x}} \tag{59}$$

For clarity, let us now change the index on the time-dependent density mode amplitude, $\dot{a}_j$, to $\dot{a}_n$. Thus,

$$\dot{a}_n \, e^{ik_n \vec{x}} = c_m \, e^{ik_m \vec{x}} \tag{60}$$

The first and most important fact to note is that, for each term c_m,

$$k_n = k_m = k_j + k_\ell \tag{61}$$

Thus, the terms must always be combined such that the growth of wavenumber index n is controlled by a combination of modes of index j and index ℓ wherein

$$n = j + \ell \tag{62}$$

Obviously, there is a whole spectrum of combinations which meet the condition of (62). In our lumped parameter representation of Fourier regimes, however, there are only two classes of groupings. Let us assume that, in all cases, the index n refers to the small size regime that is growing (that is, n is a "large" number index). By definition, both j and ℓ cannot be large or there would be no connection to the "small" wavenumber regime from which power is flowing. Therefore, the two cases are: (1) either j or ℓ is "large with the other "small" or (2) both j and ℓ are "small" but their addition makes them "large" or "approaching large".

We now see that we have a convenient way of cataloguing the two lumped parameter types of transfer process. Case (1) is "seed growth", whereas case (2) is "bifurcation growth".

For example, in the idealized limits, consider for case (1) an extremely small scale seed corresponding to an extremely large wavenumber index. Then we see that (62)

is satisfied by an expression of the form

$$n \approx j >> \ell \tag{63}$$

In the limit, this is an example of a seed "growing on itself".

On the other hand, consider an example for case (2) which might represent "true bifurcation in Fourier space".

$$n = 2j = 2\ell \tag{64}$$

Note that this process does not necessarily manifest itself as an observable "bifurcation in physical space".

The second important fact to note about the expressions (56) to (60) is the functional dependence of the growth rate (of the coefficient a_n) with respect to the other parameters

$$\dot{a}_n = (\vec{k}_j \dot{a}_j) \cdot (\vec{k}_\ell b_\ell) \tag{65}$$

We easily identify $\vec{k}_j a_j$ with the Fourier decomposition of $1/d$ and $\vec{k}_\ell b_\ell$ with (ΔU). Thus, the basic functional form of our growth rate, (51), derived for "seed growth" is probably valid for all regimes. We can assume, however, that it will not produce as rapid a flow of power out of the small k regime into the large k regime. This is merely because it has to cycle many times. That is, the intrinsic convolution process is identical, but the seed mechanism produces growth in one time cycle, whereas the bifurcation mechanism must cycle many times to increase the wavenumber substantially. Under ideal conditions, the bifurcation mechanism can only double the wavenumber each cycle.

We believe it reasonable to reduce the bifurcation rate, as compared to the seed rate, by the ratio of mean weighted wavenumber through which the cycling process must travel, $\bar{k}_m/\bar{k}_n$. Otherwise, we shall postulate that it ought to have an identical format, thus

$$R_{mn_\beta} = 2(\Delta U)\ \bar{k}_m \sqrt{\frac{L}{\pi} F_m}\ \frac{\bar{k}_m}{\bar{k}_n} F_m \qquad (66)$$

In concluding this subsection on growth rates, it is important to make several features clear. The rates have been formulated with the best current theoretical ideas and contain nothing that is known to be contradictory to the current data base on gradient drift mechanics, whether derived from experiment or numerical solution of exact plasma equations. Nonetheless, a variety of assumptions have been necessary to formulate the complete modelling. There is, thus, no guarantee that these procedures are truly correct. To compensate for the above, we shall provide for modification to the results by multiplicative, adjustable coefficients (α and β). Experience in testing and applying the model may show these to be small constant corrections of order unity on the one hand, or large perturbing functional relationships on the other hand. In any event, they will provide the vehicle through which this model can be made consistent with new theory or new data. Thus, in final form, the rates are expressed as

$$R_{mn_\alpha} = 2\alpha\ (\Delta U)\ \bar{k}_m \sqrt{\frac{L}{\pi} F_m}\ F_n \qquad (67)$$

and

$$R_{mn_\beta} = 2\beta\ (\Delta U)\ \bar{k}_m \sqrt{\frac{L}{\pi} F_m}\ \frac{\bar{k}_m}{\bar{k}_n} F_m \qquad (68)$$

C. DIFFUSION RATE

As indicated in earlier discussions, crossfield plasma diffusion is the process which completes the dynamical life cycle of the plasma evolution. It will have a significant influence only on the very smallest scale sizes (or largest wavenumbers), and, for simplicity, we will include the effect only in our defined "diffusion regime". In the simple form, to be considered here, diffusion is a purely linear process and, thus, plays no role in the cascading of wavenumbers discussed under gradient drift rates. A simple diffusion equation, that is not coupled to other plasma dynamical processes may be stated as follows

$$\frac{\partial n}{\partial t} = D \frac{\partial^2 n}{\partial \vec{x}^2} \tag{69}$$

where n is plasma density and D is the classical cross-field electron diffusion coefficient. For a plasma composed of Fourier modes of the form

$$f_n \, e^{i\theta_n} \, e^{i\vec{k}_n \cdot \vec{x}_n} \tag{70}$$

the relation (69) takes the form

$$\frac{df_n}{dt} = -k_n^2 \, D \, f_n \tag{71}$$

or equivalently (and dropping the subscript),

$$\frac{1}{2} \frac{df^2}{dt} = -D \, k^2 \, f^2 \tag{72}$$

Integrating this expression over some range in Fourier space gives

$$\frac{1}{2}\frac{d}{dt}\int f^2\,dk = -D\int k^2\,f^2\,dk \tag{73}$$

or using the definitions of (23) and (45)

$$\frac{1}{2}\frac{d\,F_m}{dt} = -D\,H_m \tag{74}$$

which is equivalent, using (46) to

$$\frac{1}{2}\frac{d\,F_m}{dt} = -D\,\bar{k}_m^2\,F_m \tag{75}$$

We then express the final form of the diffusion rate, required by the matrix of conservation relations, (30), as

$$\text{diffusion} = 2\varepsilon\,D\,\bar{k}_m^2\,F_m \tag{76}$$

where we have introduced a correction coefficient, ε, in the spirit of our other rate expressions. In practice, this correction may be useful for introducing augmented diffusion from anomalous plasma turbulence (e.g., drift waves).

D. THE WORKING EQUATIONS

In previous subsections, we have assembled enough material to now write down the basic differential equations which govern the model. Substituting the rates of form (67), (68), and (76) into (30) gives

$$\frac{1}{2}\frac{dF_O}{dt} = -(\Delta U)\,\bar{k}_O\,F_R\sqrt{\frac{L}{\pi}F_O} - \beta_1\,(\Delta U)\,\bar{k}_O\,F_O\sqrt{\frac{L}{\pi}F_O}\,\frac{\bar{k}_O}{k_R}$$
$$-(\Delta U)\,\bar{k}_O\,F_C\sqrt{\frac{L}{\pi}F_O} - (\Delta U)\,\bar{k}_O\,F_D\sqrt{\frac{L}{\pi}F_O} \tag{77}$$

$$\frac{1}{2}\frac{dF_R}{dt} = (\Delta U)\ \bar{k}_O\ F_R \sqrt{\frac{L}{\pi} F_O} - \alpha_1\ (\Delta U)\ \bar{k}_R\ F_C \sqrt{\frac{L}{\pi} F_R}$$
$$- \alpha_2\ (\Delta U)\ \bar{k}_R\ F_D \sqrt{\frac{L}{\pi} F_R} + \beta_1\ (\Delta U)\ \bar{k}_O\ F_O \sqrt{\frac{L}{\pi} F_O}\ \frac{\bar{k}_O}{\bar{k}_R}$$
$$- \beta_2\ (\Delta U)\ \bar{k}_R\ F_R \sqrt{\frac{L}{\pi} F_R}\ \frac{\bar{k}_R}{\bar{k}_C} \qquad (78)$$

$$\frac{1}{2}\frac{dF_C}{dt} = (\Delta U)\ \bar{k}_O\ F_C \sqrt{\frac{L}{\pi} F_O} + \alpha_1\ (\Delta U)\ \bar{k}_R\ F_C \sqrt{\frac{L}{\pi} F_R}$$
$$- \alpha_3\ (\Delta U)\ \bar{k}_C\ F_D \sqrt{\frac{L}{\pi} F_C} + \beta_2\ (\Delta U)\ \bar{k}_R\ F_R \sqrt{\frac{L}{\pi} F_R}\ \frac{\bar{k}_R}{\bar{k}_C}$$
$$- \beta_3\ (\Delta U)\ \bar{k}_C\ F_C \sqrt{\frac{L}{\pi} F_C}\ \frac{\bar{k}_C}{\bar{k}_D} \qquad (79)$$

$$\frac{1}{2}\frac{dF_D}{dt} = (\Delta U)\ \bar{k}_O\ F_D \sqrt{\frac{L}{\pi} F_O} + \alpha_2\ (\Delta U)\ \bar{k}_R\ F_D \sqrt{\frac{L}{\pi} F_R}$$
$$+ \alpha_3\ (\Delta U)\ \bar{k}_C\ F_D \sqrt{\frac{L}{\pi} F_C} + \beta_3\ (\Delta U)\ \bar{k}_C\ F_C \sqrt{\frac{L}{\pi} F_C}\ \frac{\bar{k}_C}{\bar{k}_D}$$
$$- \varepsilon D\ \bar{k}_D^2\ F_D \qquad (80)$$

There are, of course, a series of constitutive relations needed to complete the total set of working equations. These will be developed below using the various definitions from previous subsections.

It should be noted, in passing, that it is not the usual practice to employ Equation (77) in actual numerical simulations. Normally, the properties of the macroscale regime are computed and fed into the modelling directly from a plasma hydrodynamic code. In that usual case, the following parameters are specified as below

$$\bar{k}_O \sqrt{\frac{L}{\pi} F_O} = \frac{\nabla n}{n} \text{ (from the code)} \tag{81}$$

$$\bar{k}_O = \frac{1}{2} k_R \tag{82}$$

In application, the wavenumber k_R is fixed at the start of the calculation and not varied thereafter. It is both logical and convenient (though not mandatory), to choose this quantity as equivalent to the wavenumber associated with the characteristic minimum plasma dimension which the macroscopic code is capable of calculating.

The constitutive relations rely on the assumptions made concerning the power spectral distribution in the various regimes of Fourier space. Referring to Figure 3 for assistance, the distribution of f in the reservoir regime is constant and equal to f_R, thus

$$f(\text{reservoir}) = f_R = f_C \tag{83}$$

Likewise, in the cascade region, f is inversely proportional to wavenumber, such that

$$f(\text{cascade}) = \frac{k_D}{k} f_D$$

and

$$f_C = \frac{k_D}{k_C} f_D \tag{84}$$

Finally, in the diffusion regime, f is inversely proportional to the cube of wavenumber

$$f(\text{diffusion}) = \left(\frac{k_D}{k}\right)^3 f_D \tag{85}$$

Performing the integrals indicated in (28) with (83), (84) and (85), respectively, gives

$$F_R = f_R^2 \, (k_C - k_R) \tag{86}$$

$$F_C = f_C^2 \, k_C \, (1 - k_C/k_D) \tag{87}$$

$$F_D = \frac{1}{5} \, f_D^2 \, k_D \tag{88}$$

Likewise, using the definitions of (45) and (46) results in

$$\bar{k}_R = \left[\frac{1}{3} \, (k_C^2 + k_R^2 + k_C \, k_R) \right]^{1/2} \tag{89}$$

$$\bar{k}_C = \sqrt{k_D \, k_C} \tag{90}$$

$$\bar{k}_D = \left(\frac{5}{3} \right)^{1/2} k_D \tag{91}$$

Equation (91) completes the set of relations necessary to carry out a self-consistent, time-dependent solution for all parameters in the model.

In the usual numerical solution using the model, these are time-dependent inputs

$$\text{INPUTS:} \quad F_O \, , \; \Delta U \tag{92}$$

which produce the following time-dependent outputs

$$\text{OUTPUTS:} \quad f_R = f_C \, , f_D \, , k_C \, , k_D \, , F_R \, , F_C \, , F_D \tag{93}$$

A computer code has been developed which solves the working equations. The code is one part of a large ensemble of routines under development for computing nuclear phenomenology for military systems analysis. Neither the

details of the code nor its interaction with other related routines will be discussed in this report. In the following section, however, various outputs from the code will be displayed to illustrate the features of the theoretical model.

One final comment should be made concerning the reference length, L. This quantity sets the absolute values of the PSD and the various power spectral summations. As ultimately developed and used in the theoretical basis of the model, it is a purely arbitrary quantity. Thus, at this point, we are actually free to specify it as much, much larger or much, much smaller than any other dimension in a real problem. It must be fixed and constant in any given computation, however.

The PSD parameter that we shall always display is the dimensionless quantity, f^2. In displaying experimental data, however, one frequently encounters the expression "power-per-unit wavenumber". It is convenient to have our result identical, from a numerical standpoint, to this conventional quantity. This equivalence will occur if we scale our parameters to have an "apparent fundamental wavenumber of unity". That is, if the numerical problem is constructed using kilometers as a basic dimension (the usual case for us), the wavenumbers will be expressed as inverse kilometers. We, then, wish to scale such that the apparent fundamental wavenumber is <u>one</u> inverse kilometer. Notice, however, that this specification has <u>nothing</u> to do with any actual characteristic dimension in the problem.

If the fundamental wavenumber is unity, then the corresponding fundamental Fourier length is 2π, therefore we set

$$2L = 2\pi \tag{94}$$

Explicitly, in the working equations, the specification (94) simplifies rate parameters of the form

$$\sqrt{\frac{L}{\pi} F_m} = \sqrt{F_m} \tag{95}$$

Unless otherwise indicated, we shall always use this specification both in the model and in displaying numerical results.

IV. EXAMPLE CALCULATIONS AND RESULTS

Initially we will carry out a series of three runs with constant input conditions to demonstrate that the model will always achieve the identical saturated state regardless of initial conditions.

Consider a macroscale density gradient of 100 km, which is driven by a wind of 1 km/sec. For convenience, we place the leading edge of the microstructure model at $k_R = 10^{-1}$ inverse kilometers (corresponding to a plasma code mesh dimension of 62.8 km). All result plots will show the dimensionless PSD, f^2, along the vertical axis. The horizontal axis is wavenumber in inverse kilometers. Recall that our PSD is equivalent, numerically, to power-per-unit wavenumber (in kilometers). In case 1, we place no power in the microstructure model to begin. Figure 4A shows the initial condition to be a blank.

Rather rapidly, however, power flows into the model and by 10 seconds, as shown in Figure 4B, measurable power is present. Note that, initially, only a reservoir and diffusion zone are created. This feature has proven typical of highly transient states. By 30 seconds, Figure 4C, we obtain the first evidence of a cascade zone and by 60 seconds, Figure 4D, this regime is pronounced. At 100 seconds, Figure 4E, the cascade is becoming dominant, which is typical of the approach to saturation. By 400 seconds, Figure 4F, we are close to complete saturation. The spectrum will change very little from here on, no matter how long we run the program.

Saturation corresponds to a cascade process that is completely in "balance". That is, power flowing in from the macroscale, below k_R, has become identical to the

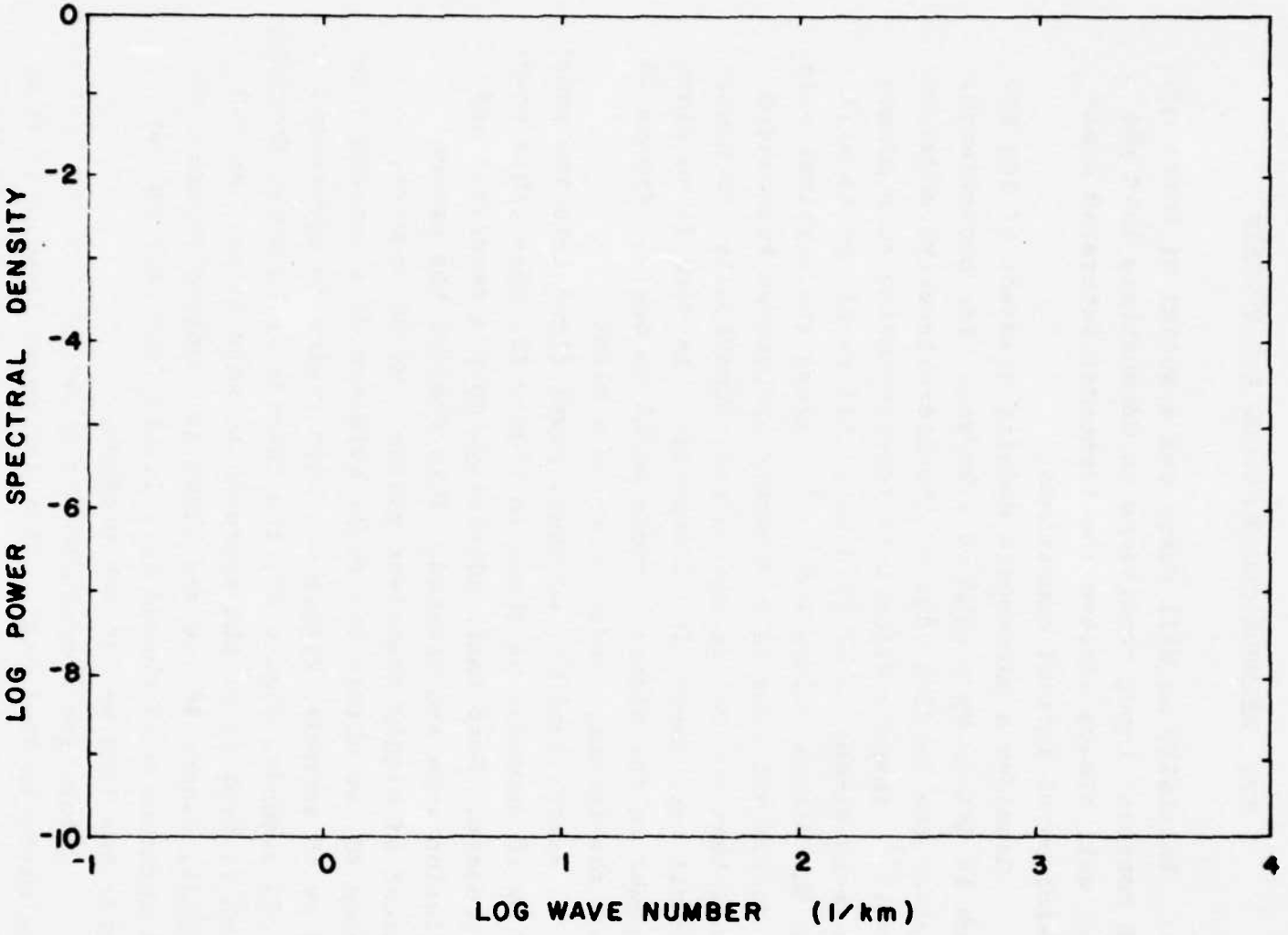

Figure 4A. Power spectrum, case 1, 0 seconds.

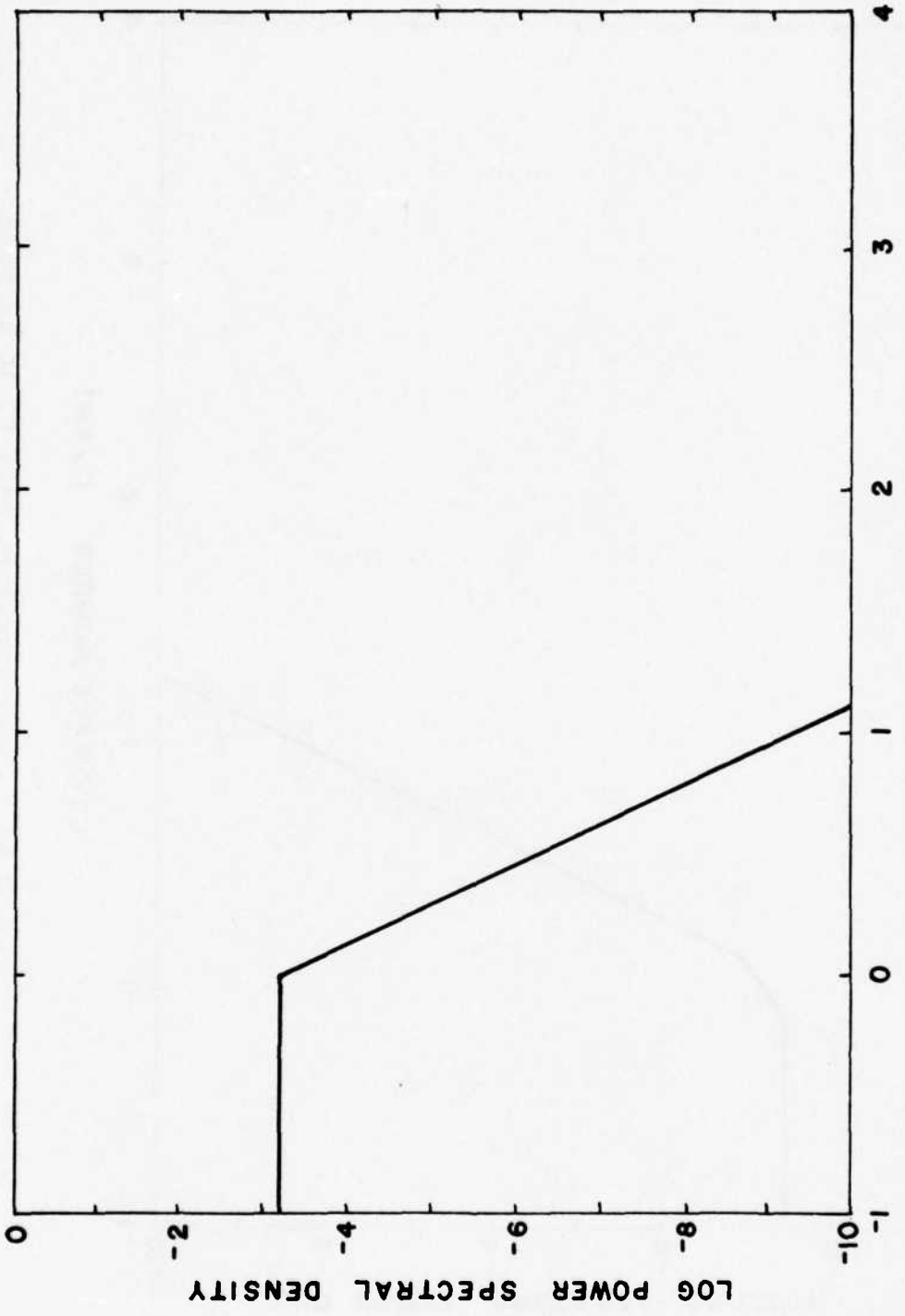

Figure 4B. Power spectrum, case 1, 10 seconds.

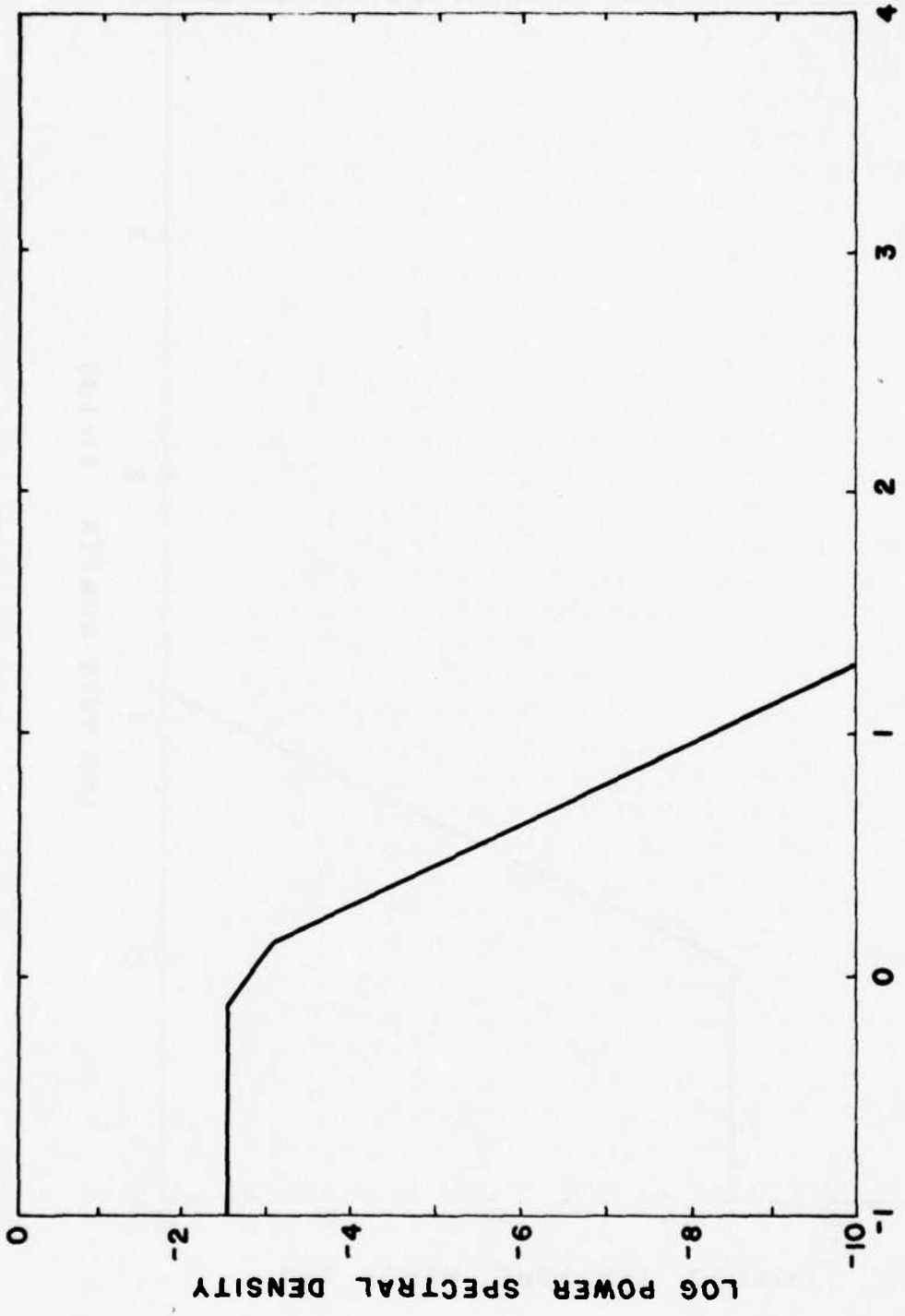

Figure 4C. Power spectrum, case 1, 30 seconds.

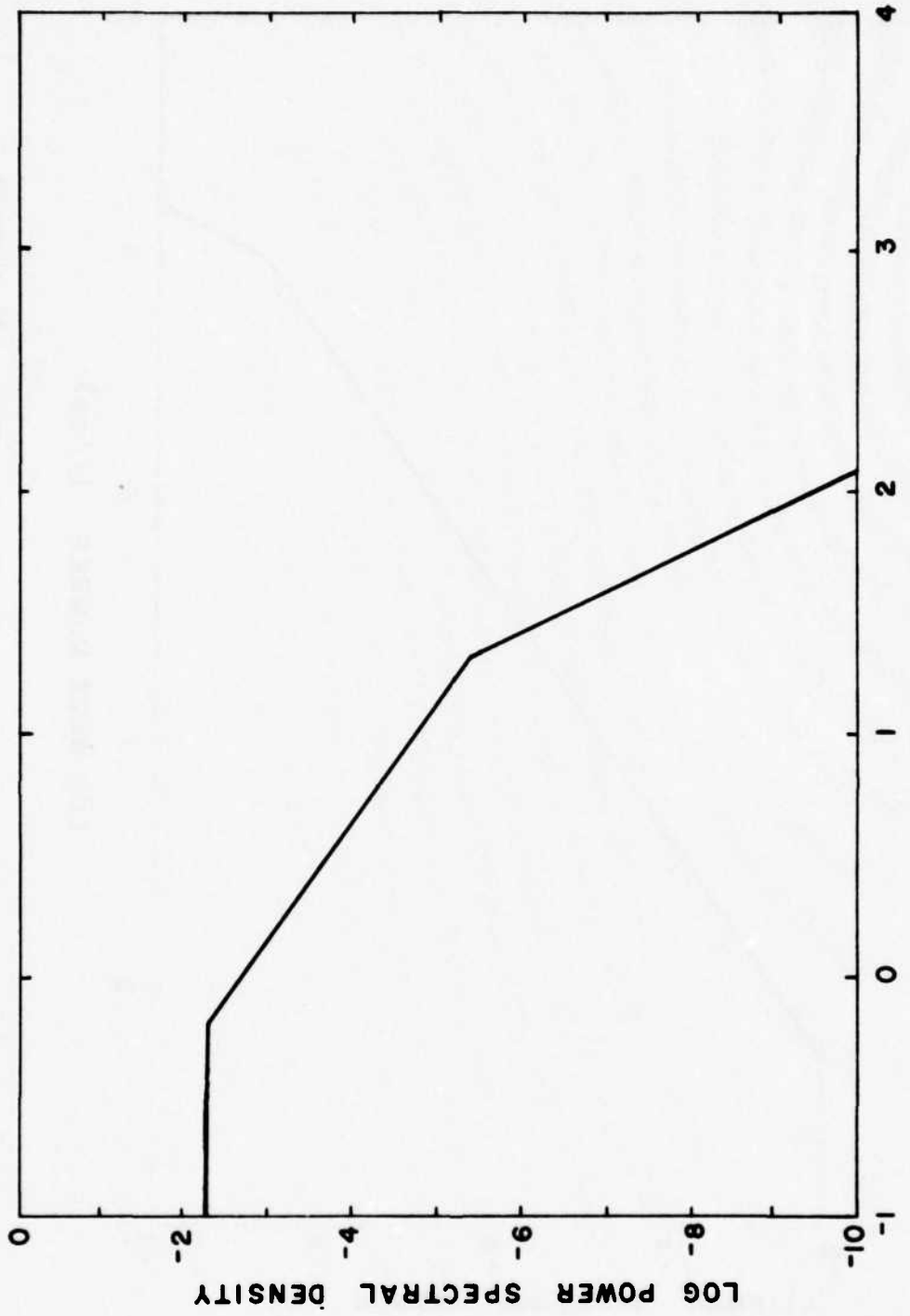

Figure 4D. Power spectrum, case 1, 60 seconds.

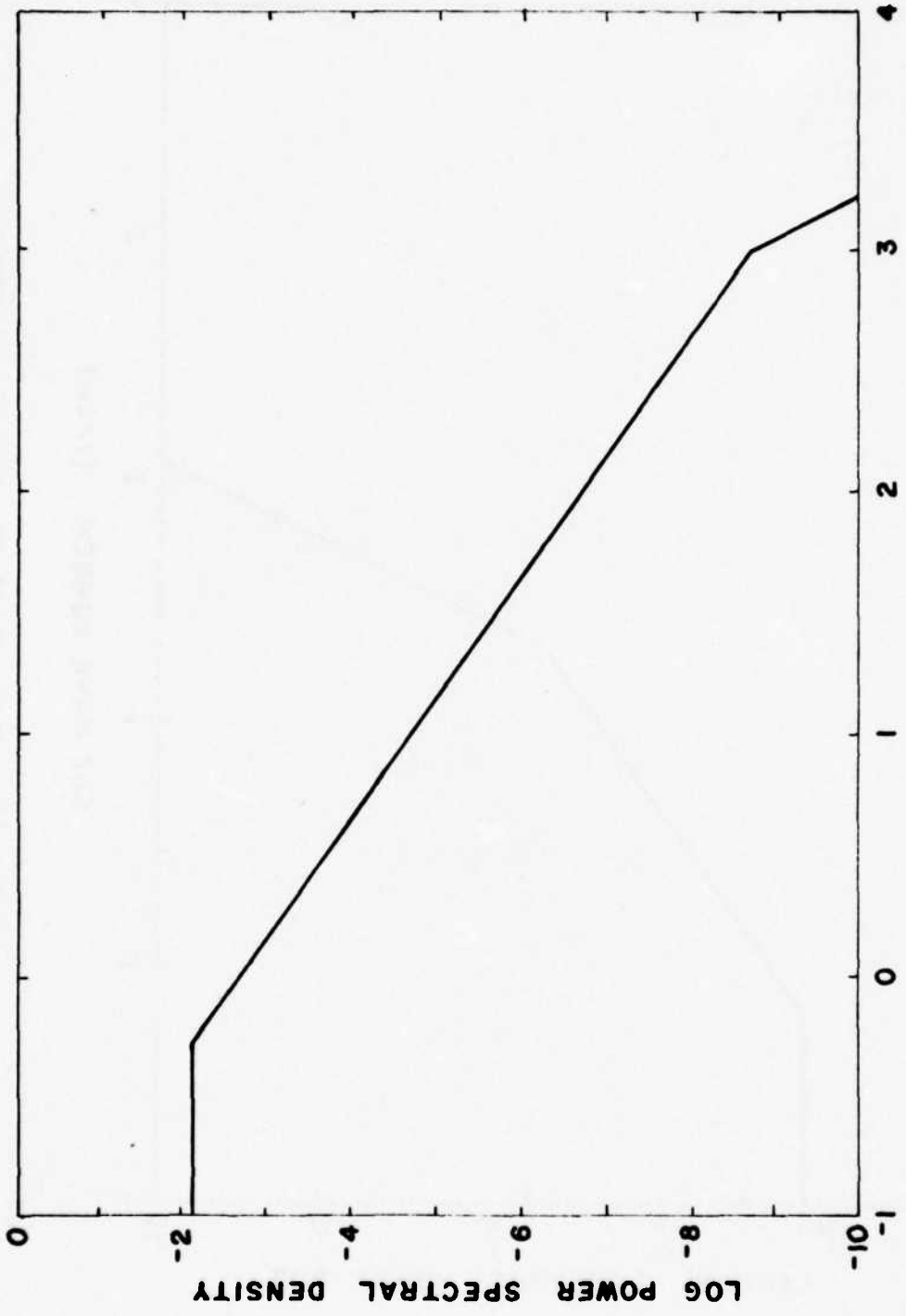

Figure 4E. Power spectrum, case 1, 100 seconds.

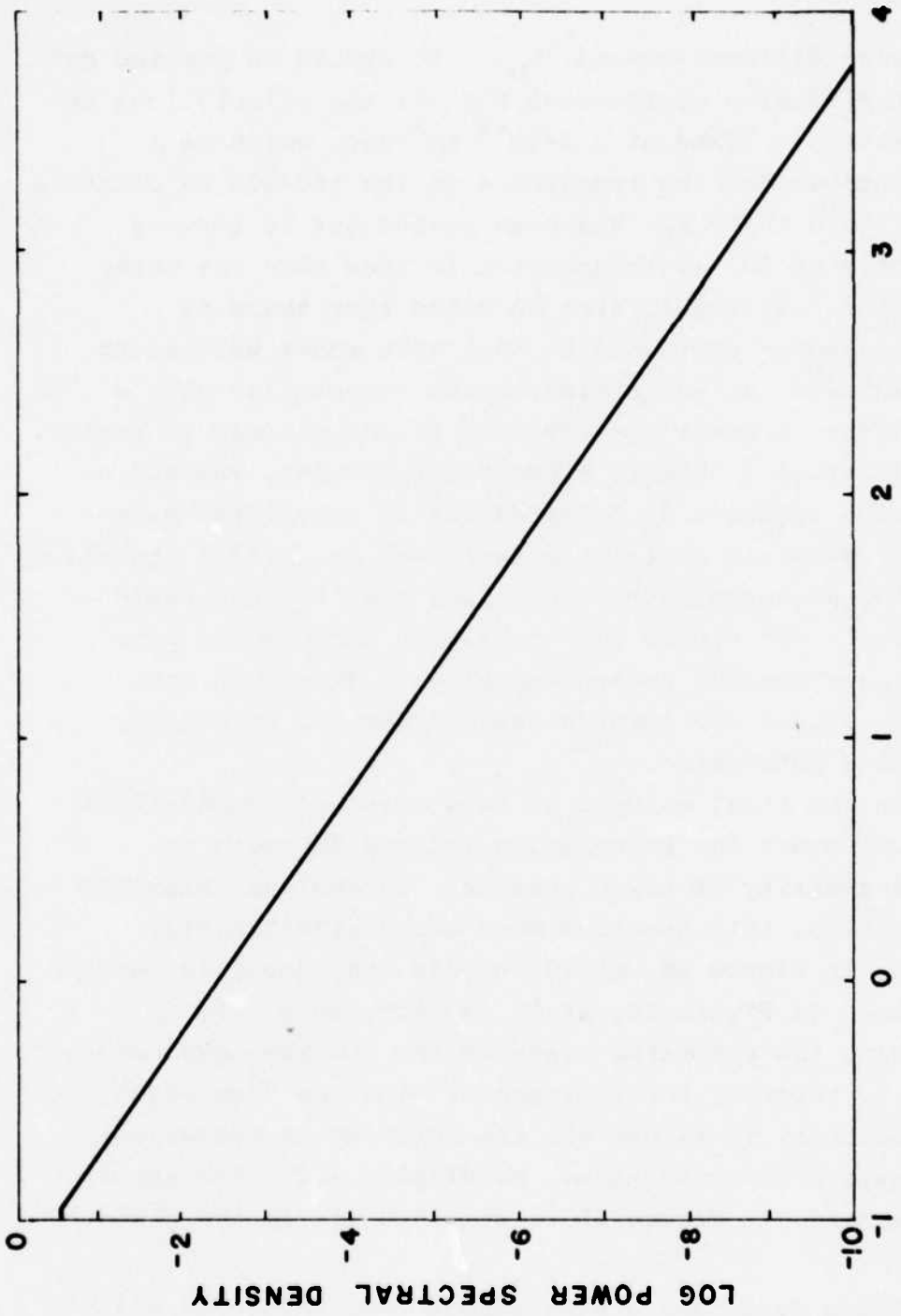

Figure 4F. Power spectrum, case 1, 400 seconds.

power being diffused beyond k_D. It should be pointed out that the diffusion coefficient for all the calculations to be presented is fixed at 2.5×10^{-5} km^2/sec, which is a nominal number for the ionosphere in the 180-200 km altitude regime. Note that k_D has been pushed out to inverse wavenumbers of 10^4 (corresponding to less than one meter wavelength). It should also be noted that there is negligible power contained at that very short wavelength.

In case 2, we initialize the computation with a quite different power distribution in the microscale regime. Figure 5A shows a "highly seeded" arrangement, wherein a flat, noise spectrum is inserted out to very large wavenumbers. We would anticipate that such an initial condition will allow an approach to saturation that is more rapid than case 1. In Figure 5B, at only 10 seconds, we note that a large cascade region has already developed and, in Figure 5C, at 200 seconds the computation is rapidly approaching saturation.

In the final example of this class of computations, case 3, we start the calculation (Figure 6A) with an enormous quantity of power present. To achieve "balance" or saturation, this spectrum must decay significantly. Note that in Figure 6B, at 10 seconds, the decay is rapidly occurring. In Figure 6C, at 50 seconds, this case is approaching the saturated state of the two previous cases. In case 3, however, the approach is from the "top side". At 200 seconds, in Figure 6D, the spectrum is essentially at an equilibrium condition. We display a further result at 300 seconds in Figure 6E to show how little the picture changes.

Cases 1, 2, and 3 demonstrate that the model will produce a common saturated spectrum starting from widely

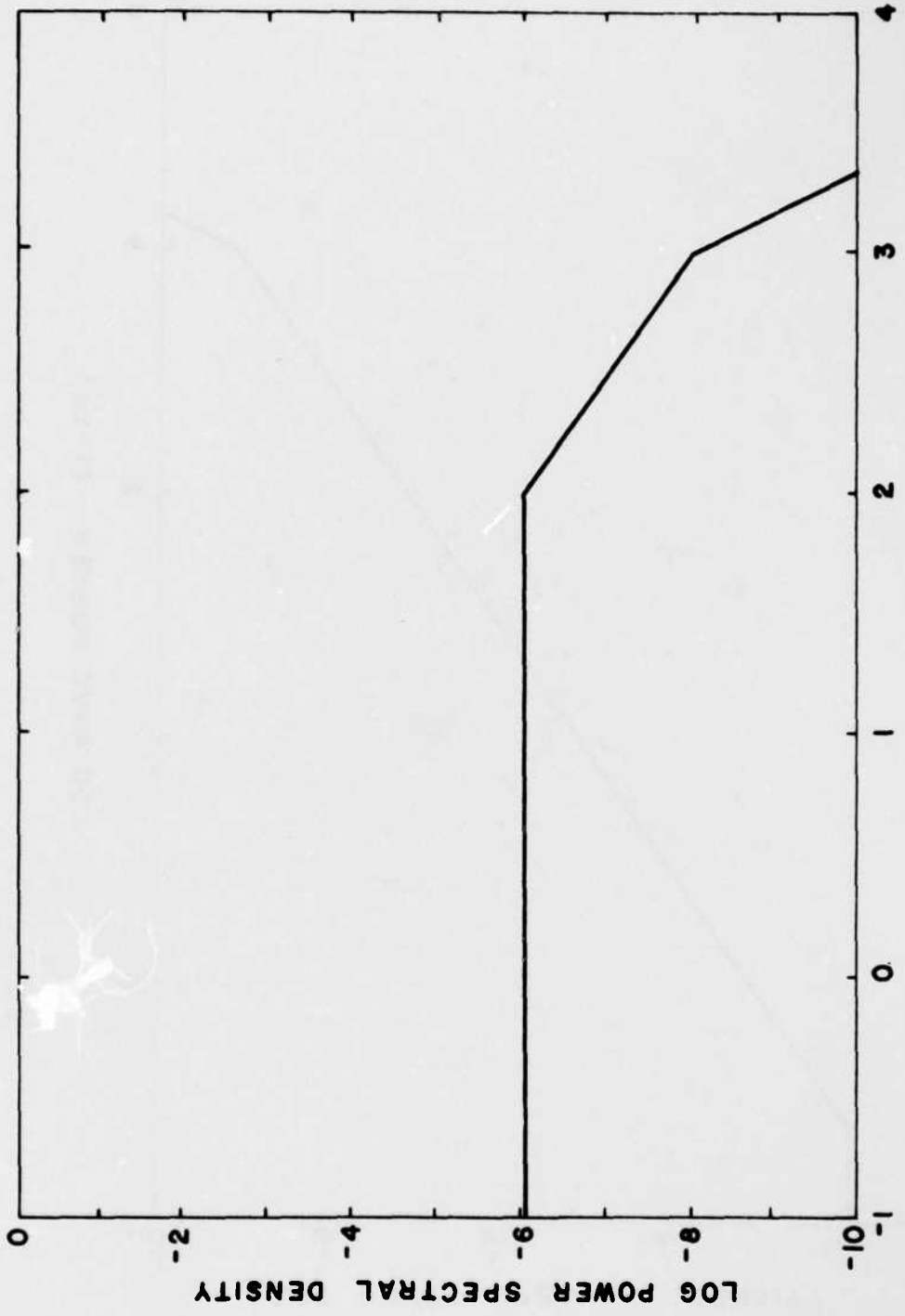

Figure 5A. Power spectrum, case 2, 0 seconds.

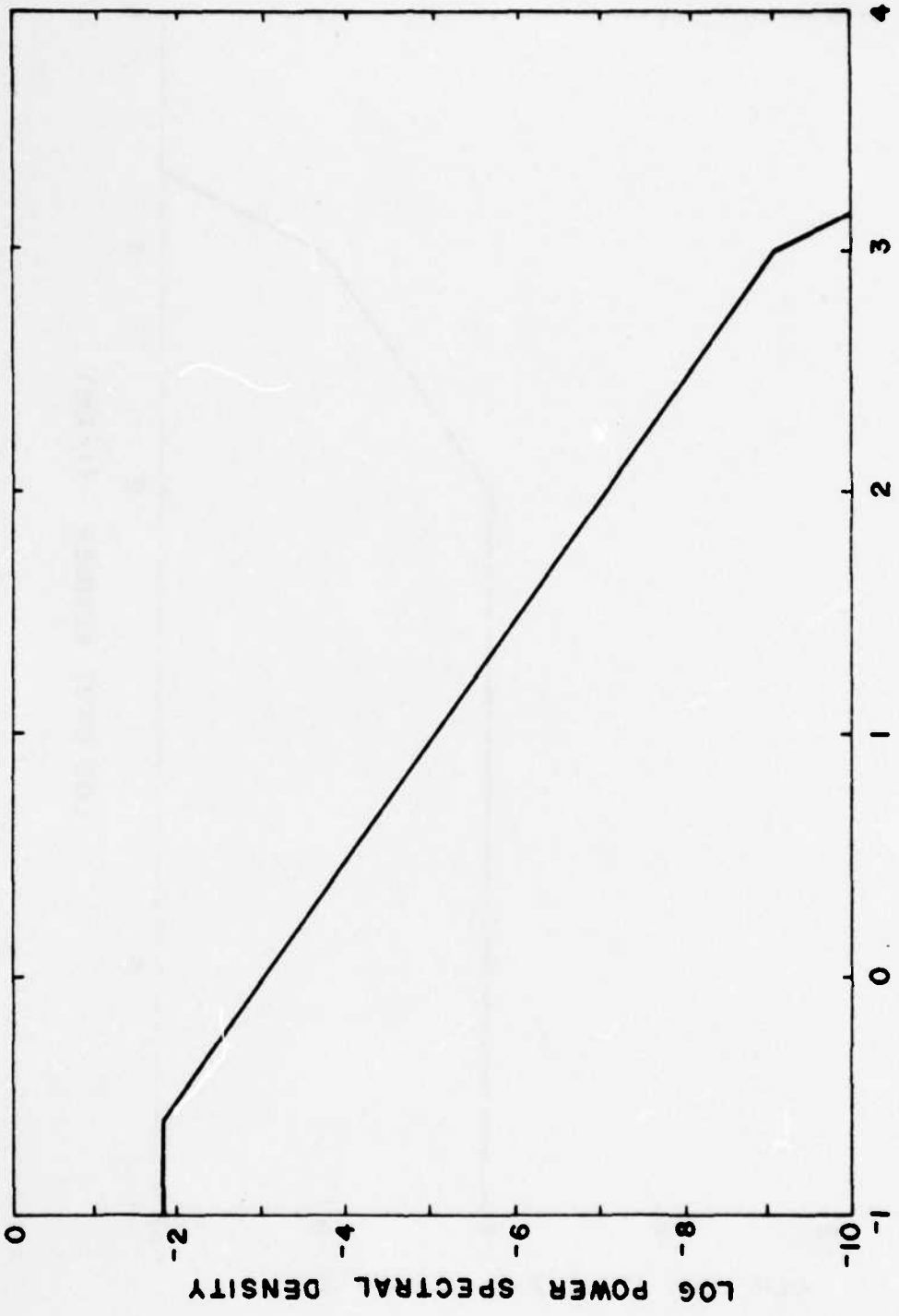

Figure 5B. Power spectrum, case 2, 10 seconds.

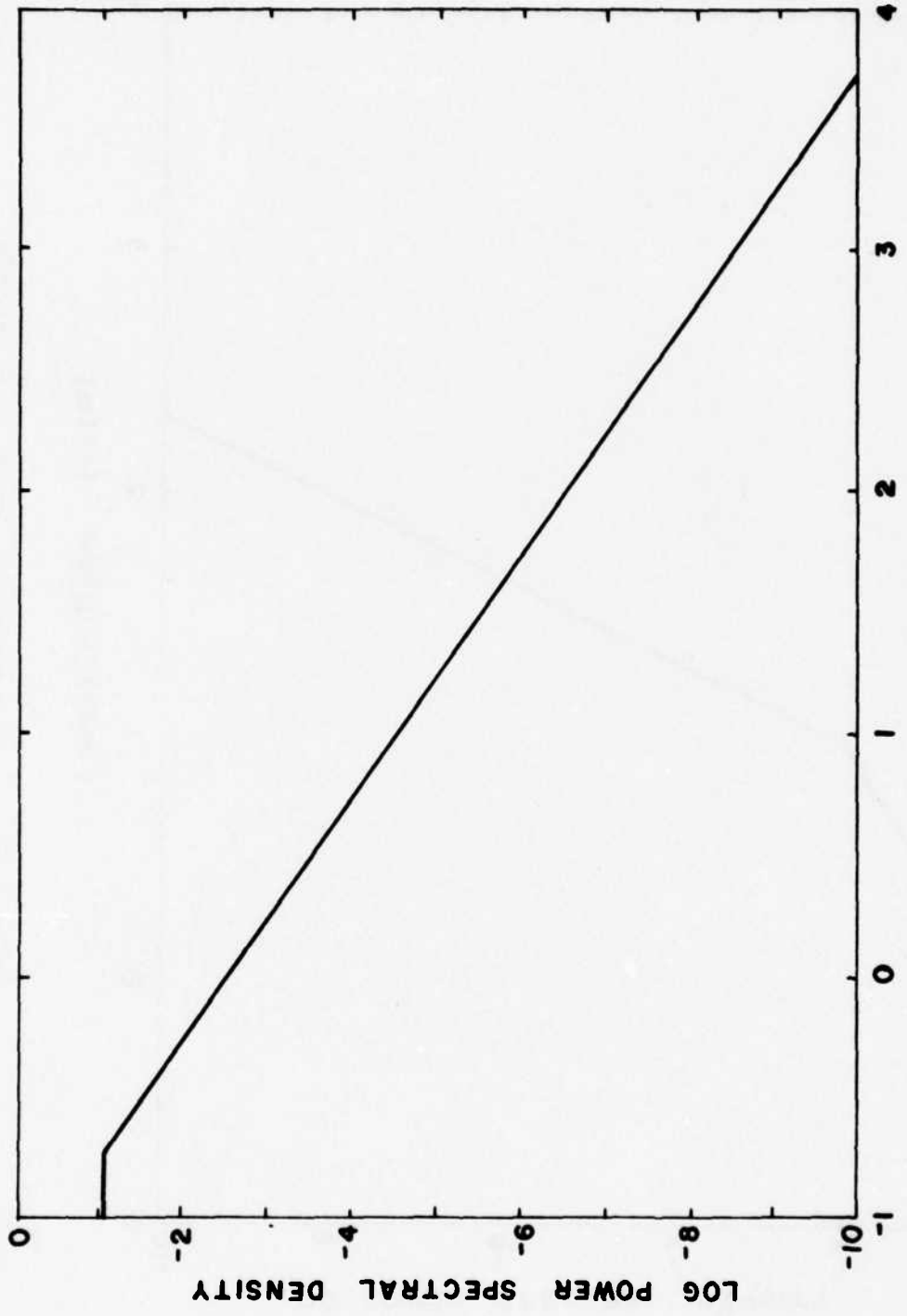

Figure 5C. Power spectrum, case 2, 200 seconds.

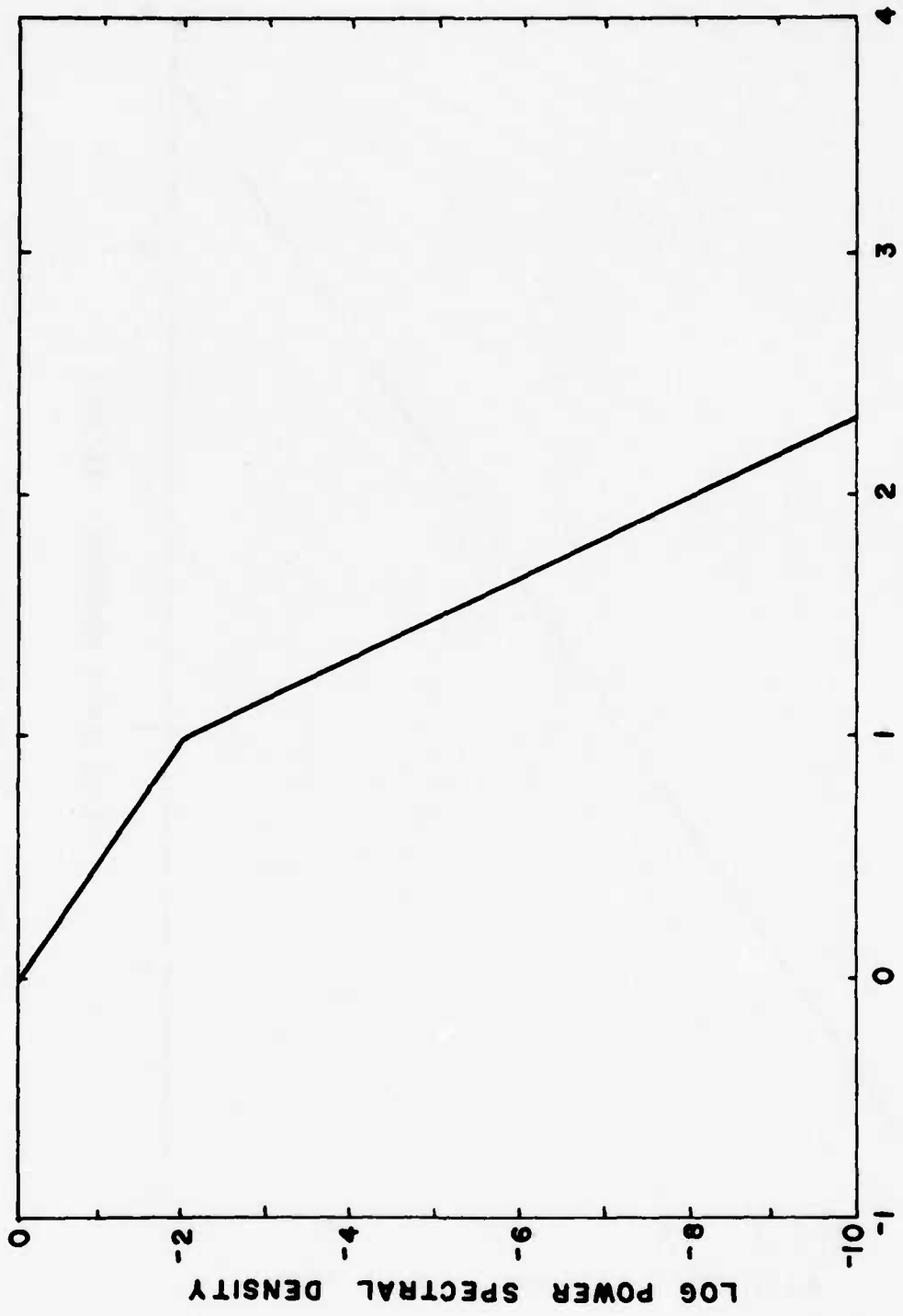

Figure 6A. Power spectrum, case 3, 0 seconds.

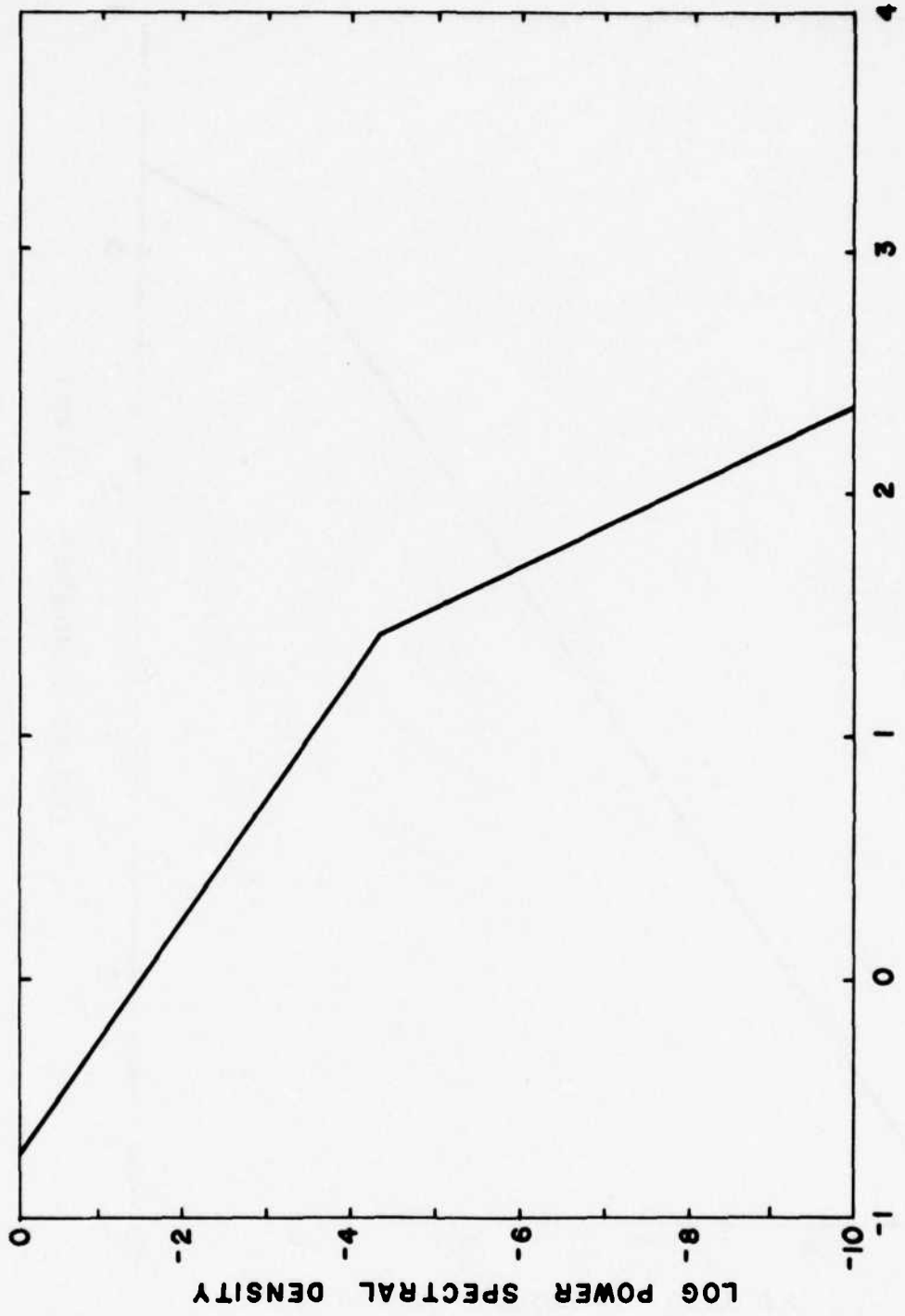

Figure 6B. Power spectrum, case 3, 10 seconds.

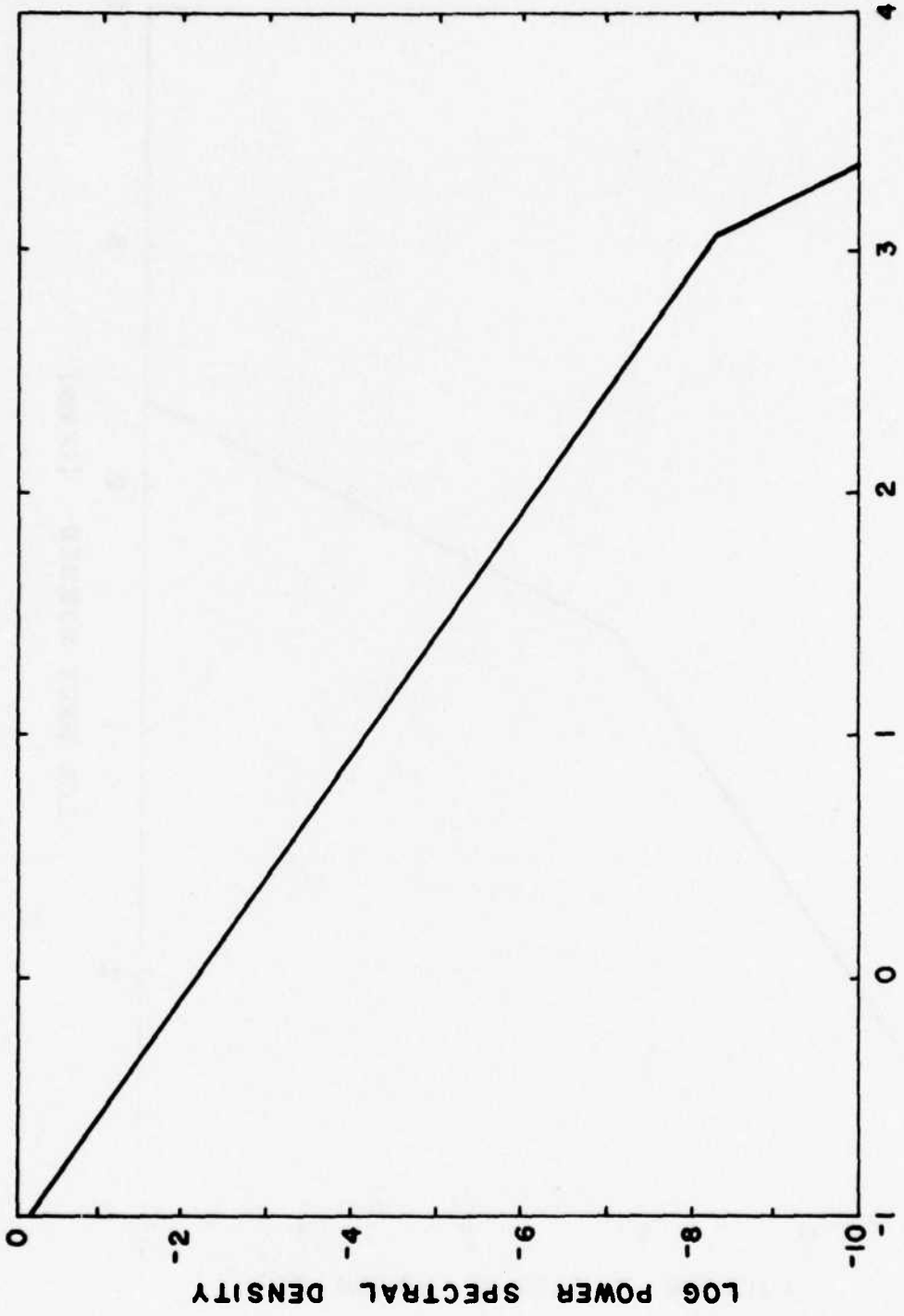

Figure 6C. Power spectrum, case 3, 50 seconds.

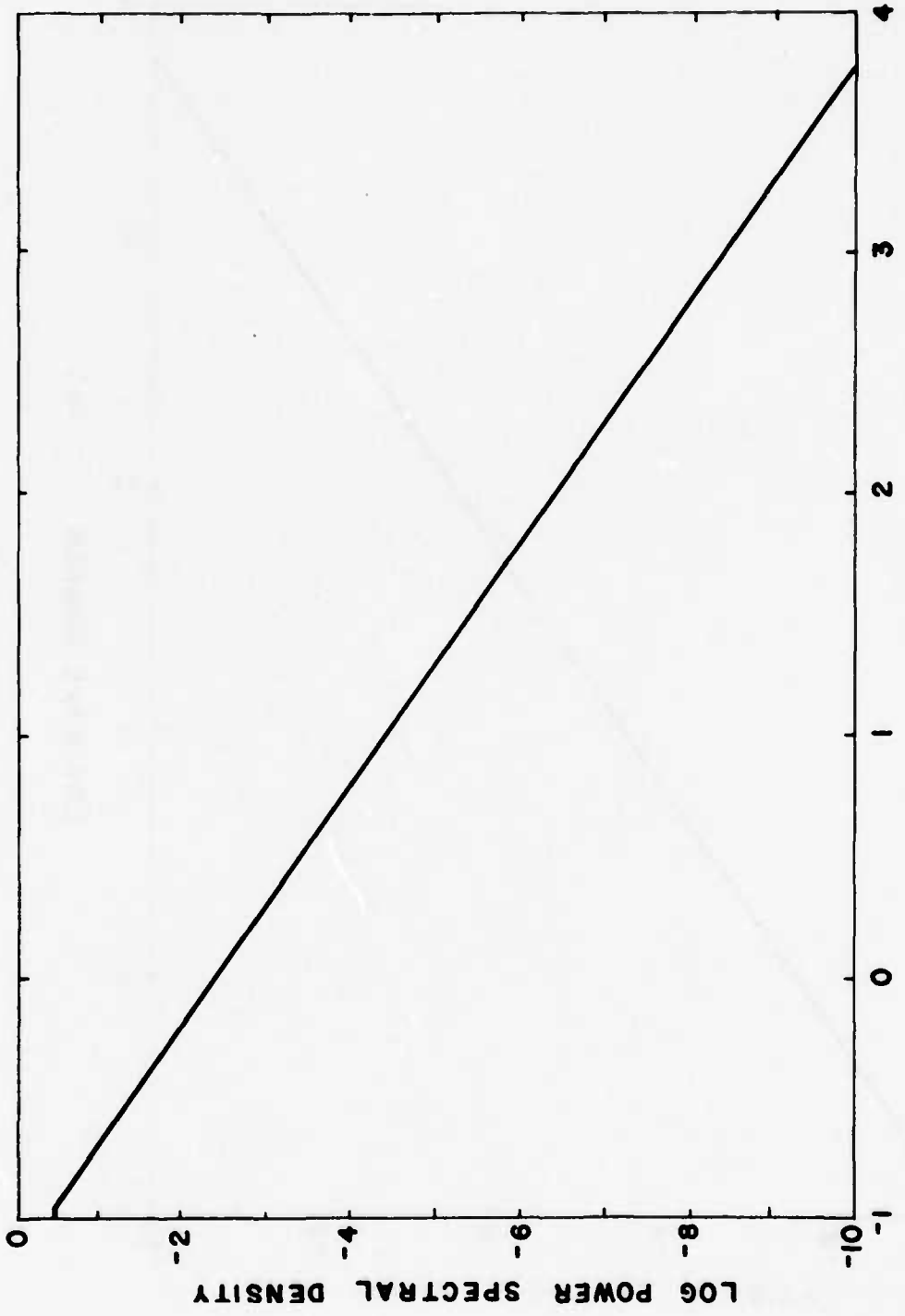

Figure 6D. Power spectrum, case 3, 200 seconds.

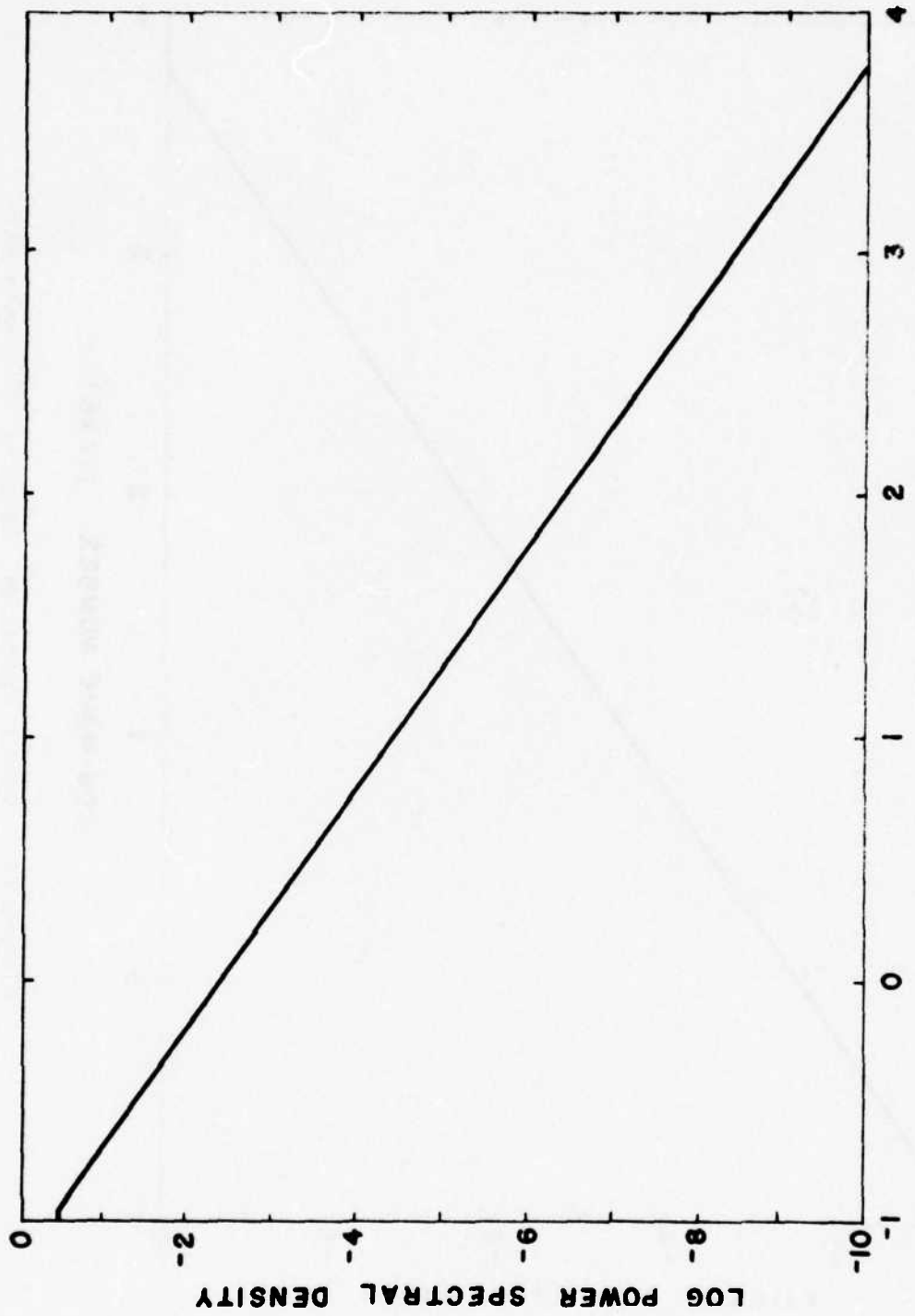

Figure 6E. Power spectrum, case 3, 300 seconds.

diverse initial conditions. It likewise demonstrates that most of the power will end in the "cascade region" if a constant driver is allowed to act for a long period of time. The only distinction among these three cases, ultimately, is in the time required to reach saturation.

Persistent saturation at high levels of power is not a realistic steady-state picture, however. Neither the wind nor the gross macroscale gradient, through which the wind blows, is going to last forever. It is interesting at this point to show the effect of removing each of these driving effects separately.

Case 4, as shown in Figure 7A, begins with the former saturated state as an initial condition. Now, however, the wind has been turned off. There is no further cascade and only diffusion is an operative mechanism. By 10 seconds, as shown in Figure 7B, decay has begun on the large wavenumbers. By 50 seconds, as in Figure 7C, the diffusion has eaten up a considerable volume of high k power. By 100 seconds, Figure 7D, the process has progressed about as far as it can go. Note that by 200 seconds, as shown in Figure 7E, there is very little change over the previous result. Of central importance is the fact that diffusion is doing nothing to get rid of the larger size structure (low k).

A more realistic, dynamic decay can be simulated if we maintain the wind, but allow the driving gradient to disappear. The initial F_0, that we employed in all of the previous cases, was a constant .04/km, corresponding to a gross gradient dimension of 100 km. The appearance of strong microstructure will destroy this gradient through the process of striation convection. We can simulate the effect by including Equation (77) in our set of relations that is time stepped.

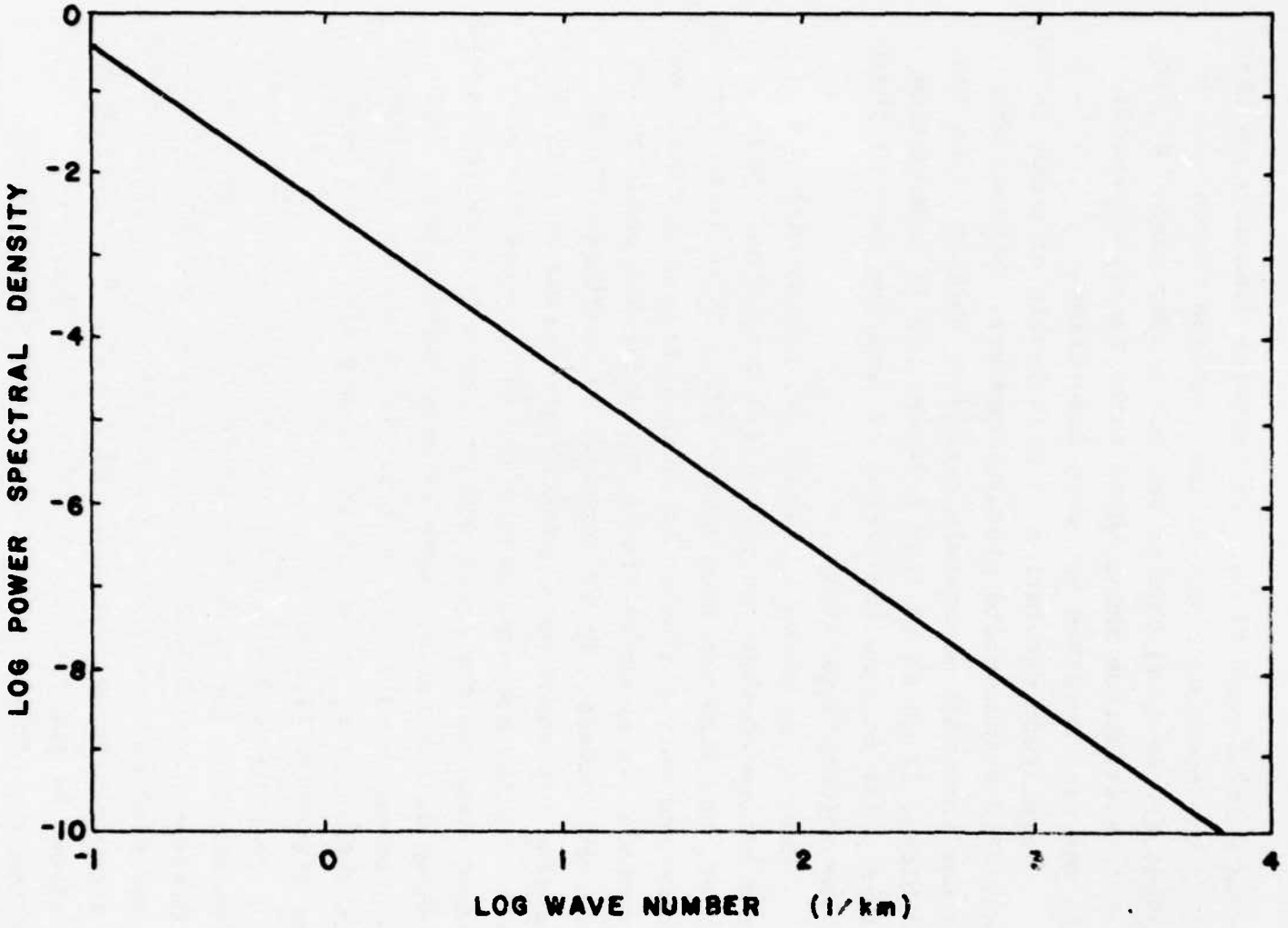

Figure 7A. Power spectrum, case 4, 0 seconds.

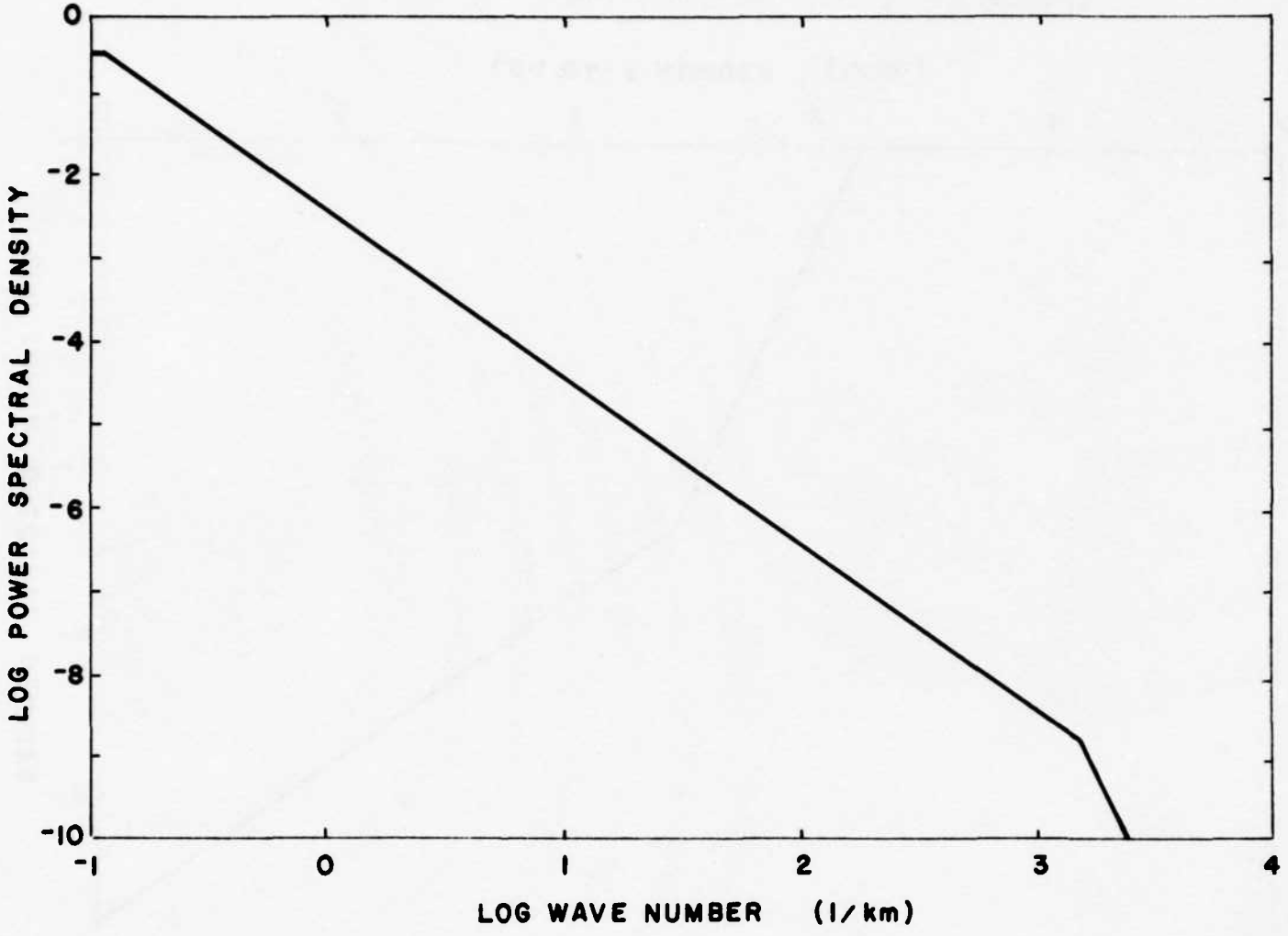

Figure 7B. Power spectrum, case 4, 10 seconds.

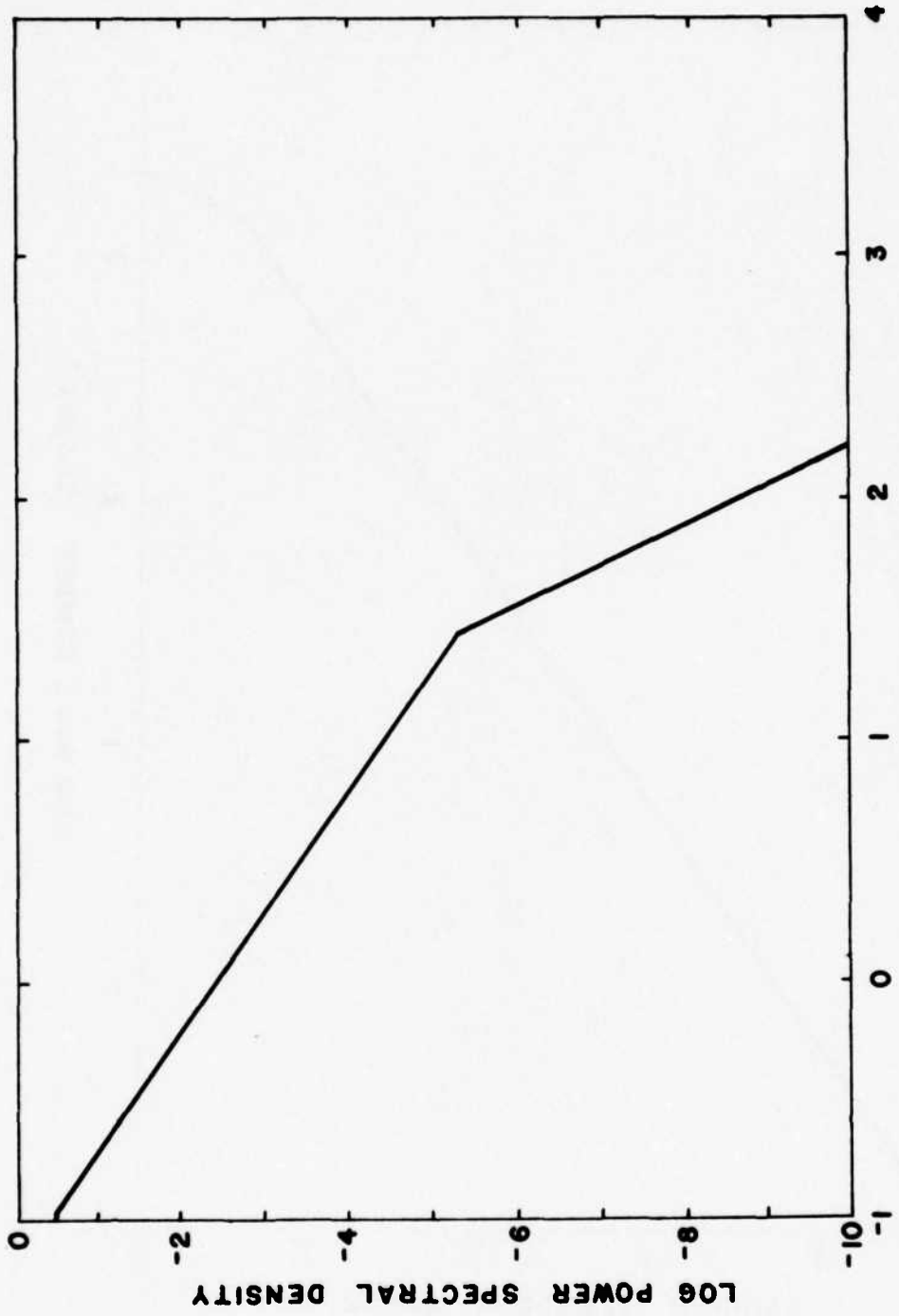

Figure 7C. Power spectrum, case 4, 50 seconds.

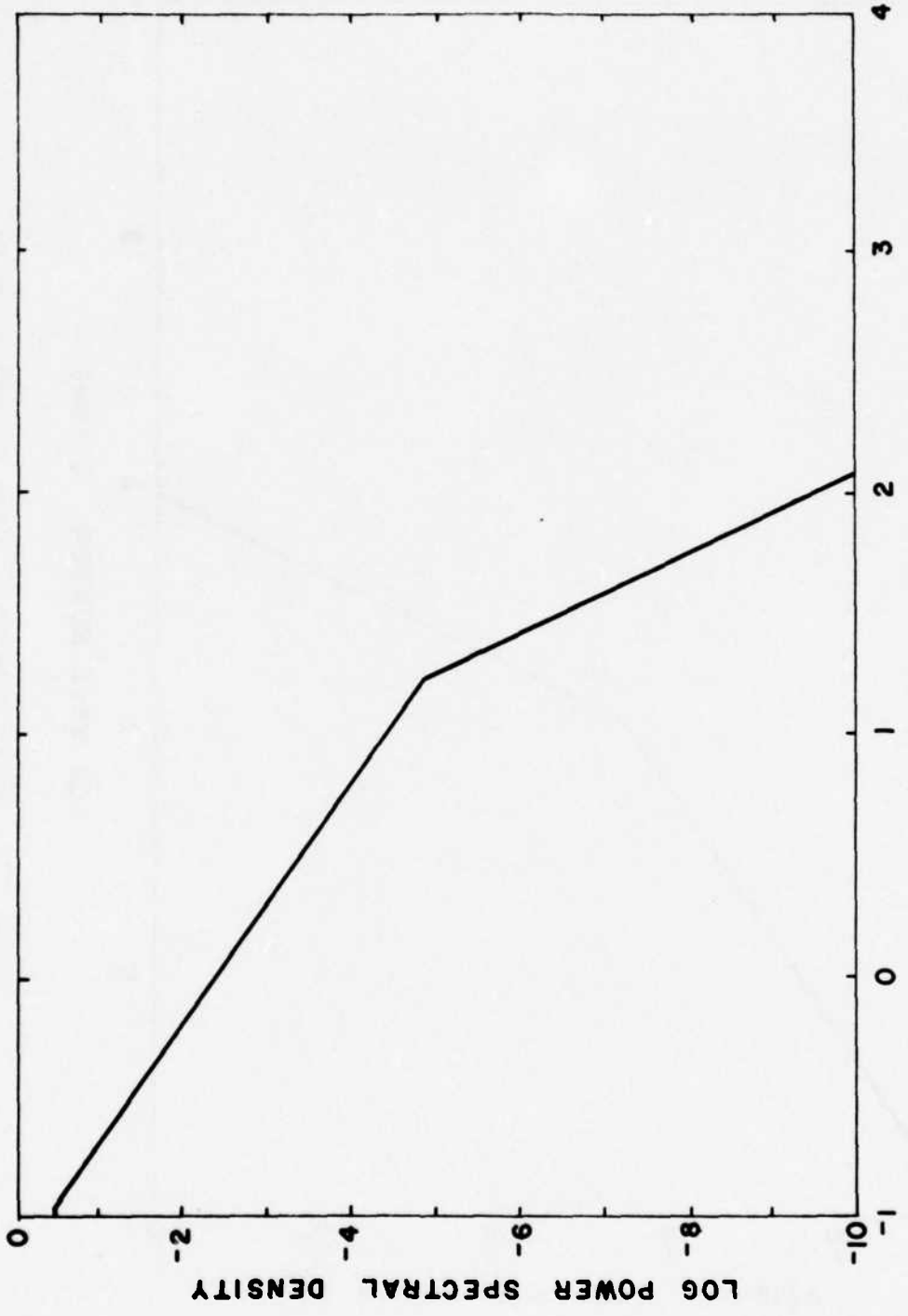

Figure 7D. Power spectrum, case 4, 100 seconds.

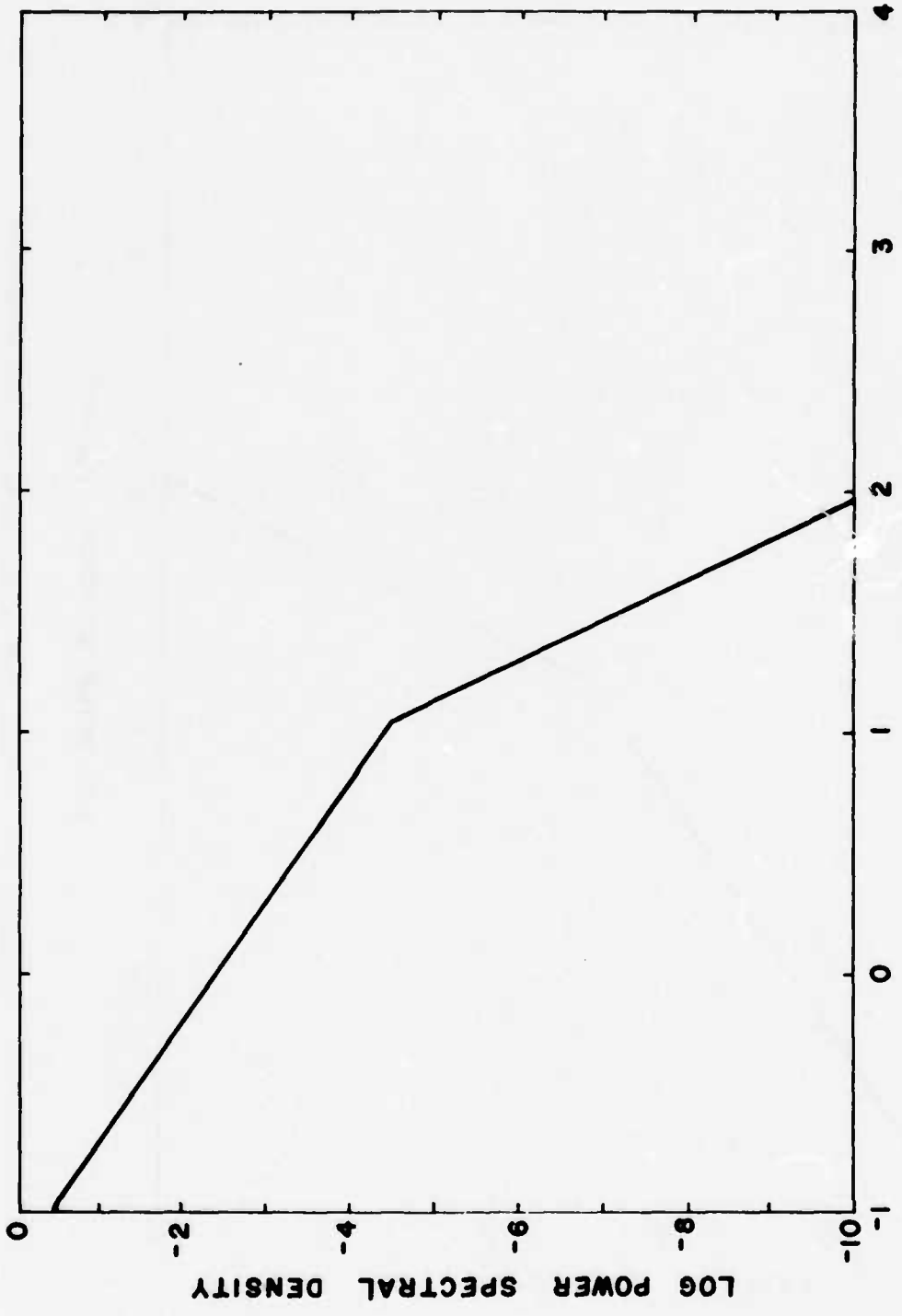

Figure 7E. Power spectrum, case 4, 200 seconds.

Let us begin case 5, as in Figure 8A, by using the final spectrum from case 4. We turn the 1 km/sec wind back on, but now allow the driving gradient F_o to decay using (77). In Figure 8B, at 50 seconds, we note that the wind is already pushing the spectrum back to the familiar saturated state, as shown in Figure 6E. This process tends to "peak out" around 100 seconds, Figure 8C. In Figure 8D, at 150 seconds, we note the push to high k values for the cascade region is running out of steam and some retreat is now evident. This effect coincides with a noticeable decline in the PSD along the leading edge at k_R.

The interesting effect, that has begun to occur strongly after 150 seconds for case 5, is the significant decay in the gross gradient (as measured by F_o).

Figure 8E is a display of F_o, corresponding to the plasma power in the macroscale regime. Notice that just prior to 200 seconds, the power is essentially all removed. Beyond this time, there is negligible power left in the macroscale to "feed" the microscale. Thus, the computation can no longer support (in quasi-equilibrium) the large diffusion implied by the combination of an extended cascade and high PSD levels. The withdrawal of the power spectrum, to lower k values, in an attempt to establish a new quasi-equilibrium is maximum about 200 seconds, as shown in Figure 8F.

As the PSD along k_R decays, the cascade is able to organize itself again and overcome some of the diffusion effect. This is primarily because the rates are quadratic in F and the transfer of power from cascade to diffusion is proportionally reduced. At 250 seconds, in Figure 8G, we see much of the cascade reasserting itself at the new, lower PSD levels. Recall that, by this time, the

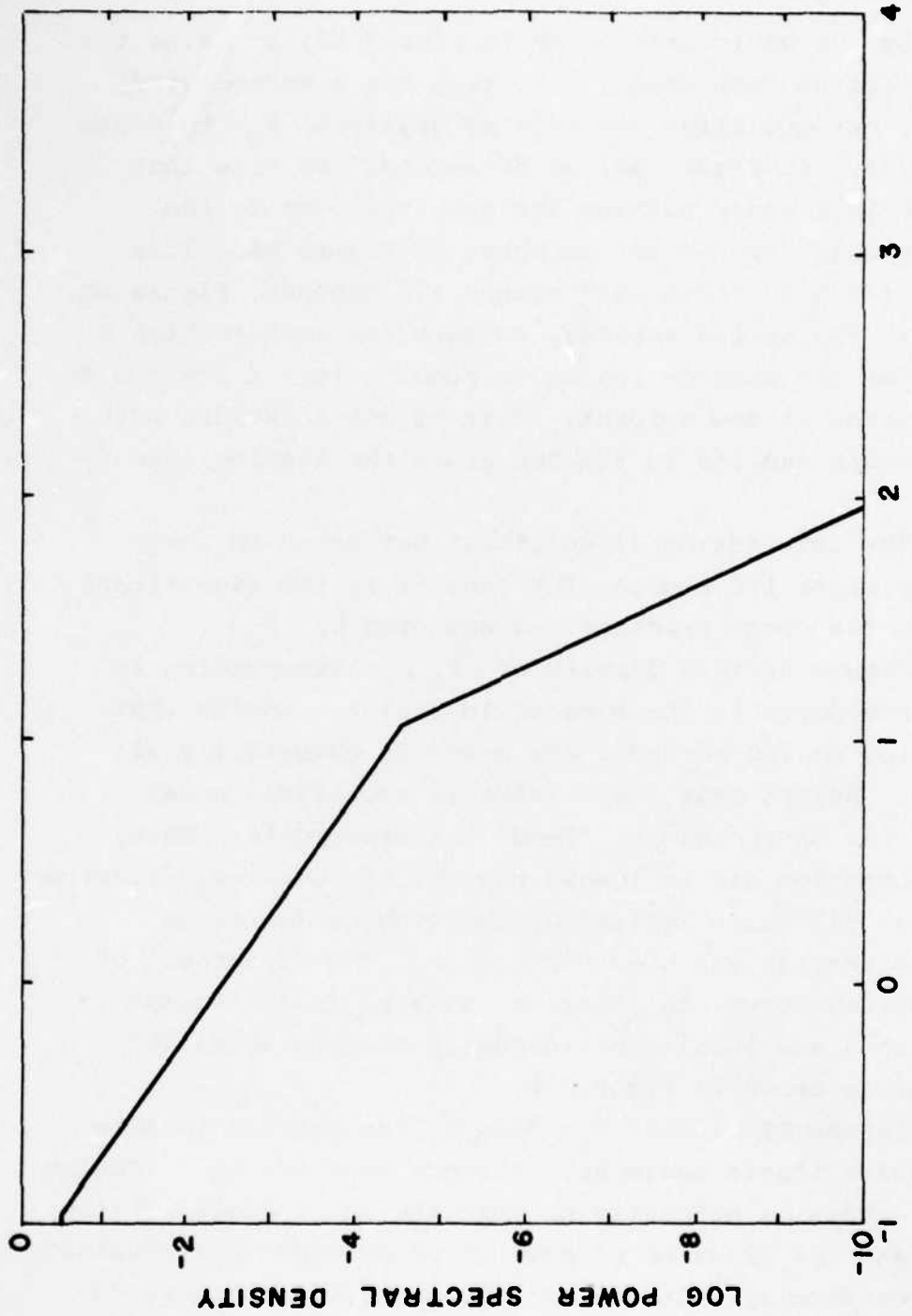

Figure 8A. Power spectrum, case 5, 0 seconds.

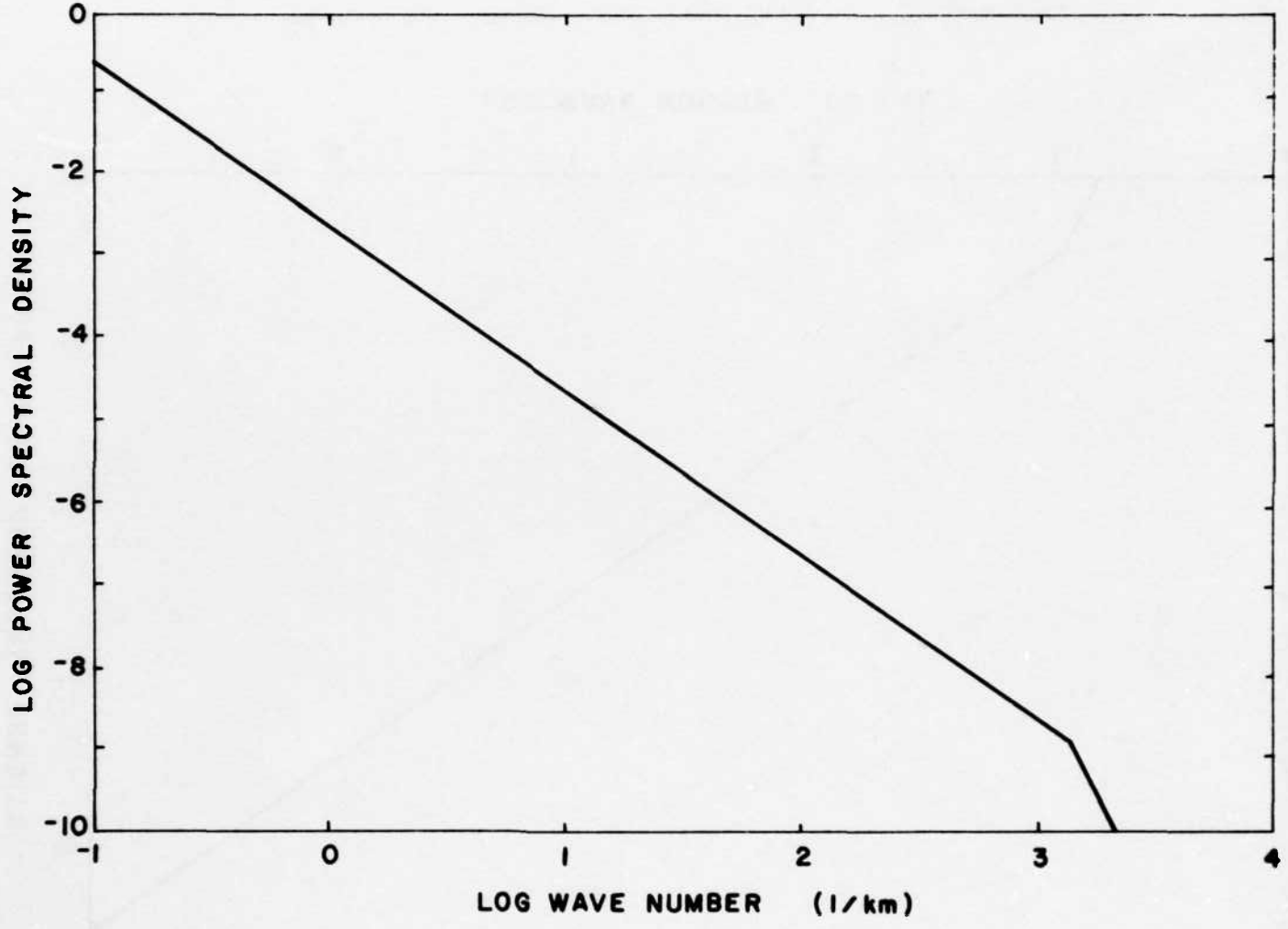

Figure 8B. Power spectrum, case 5, 50 seconds.

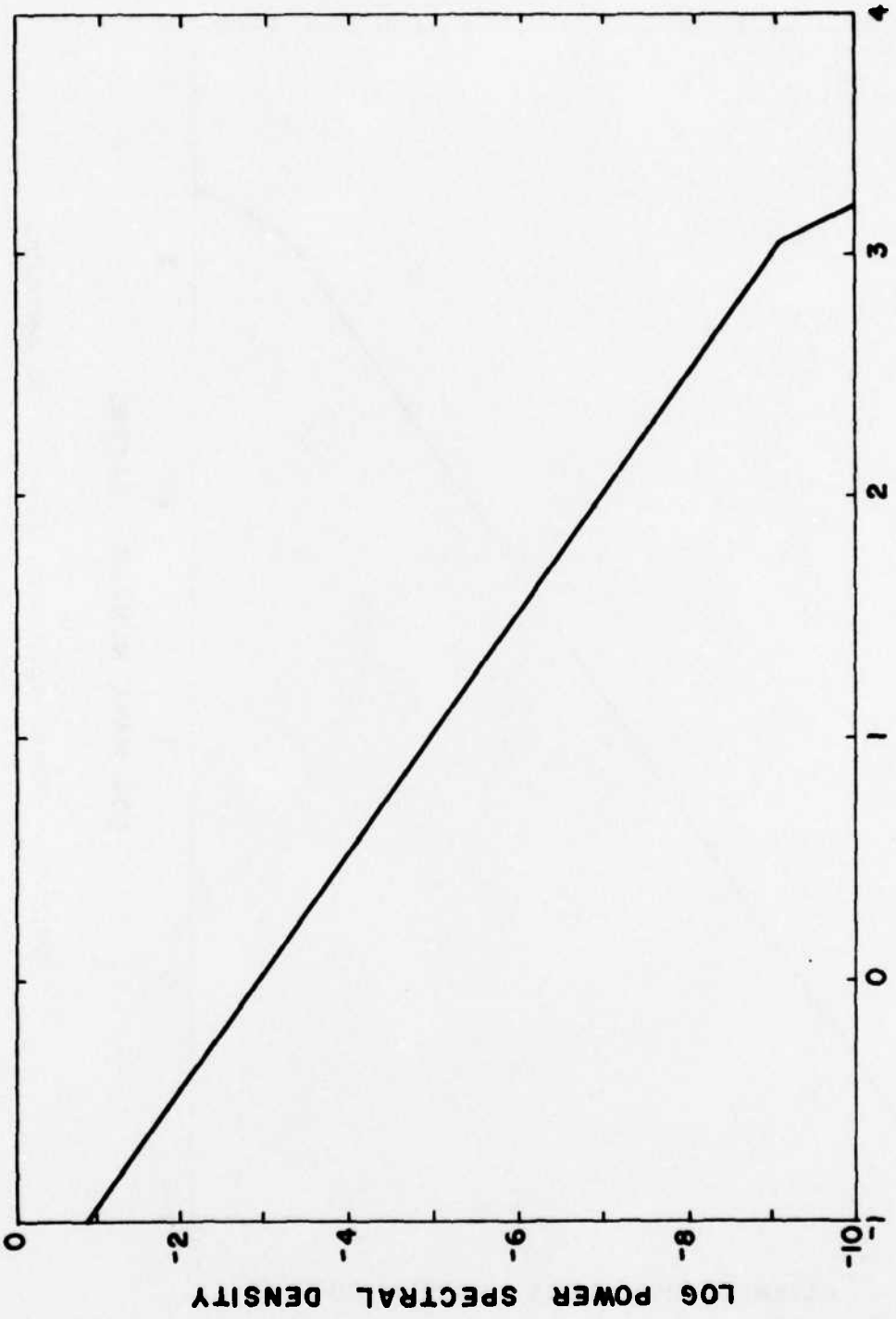

Figure 8C. Power spectrum, case 5, 100 seconds.

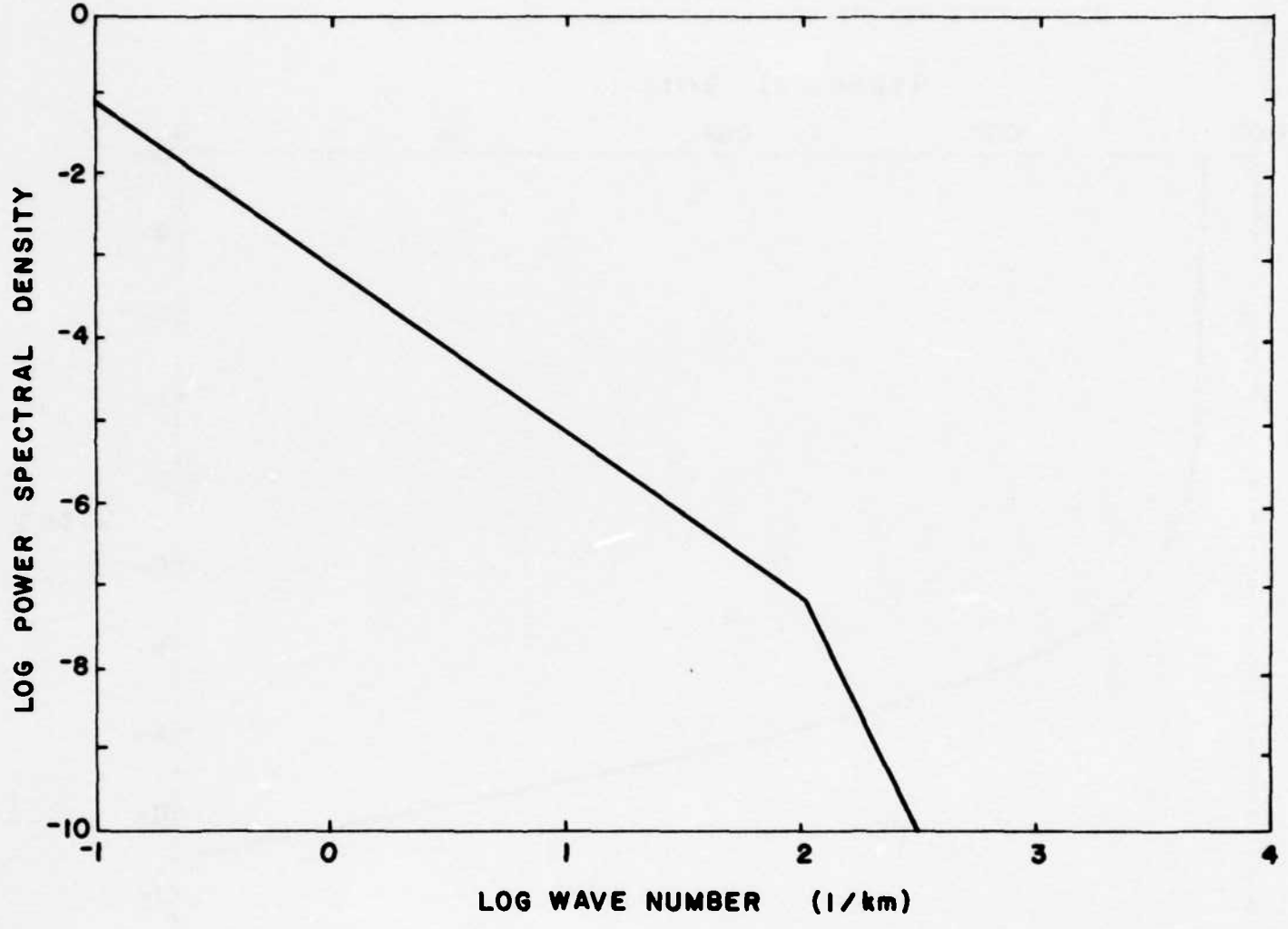

Figure 8D. Power spectrum, case 5, 150 seconds.

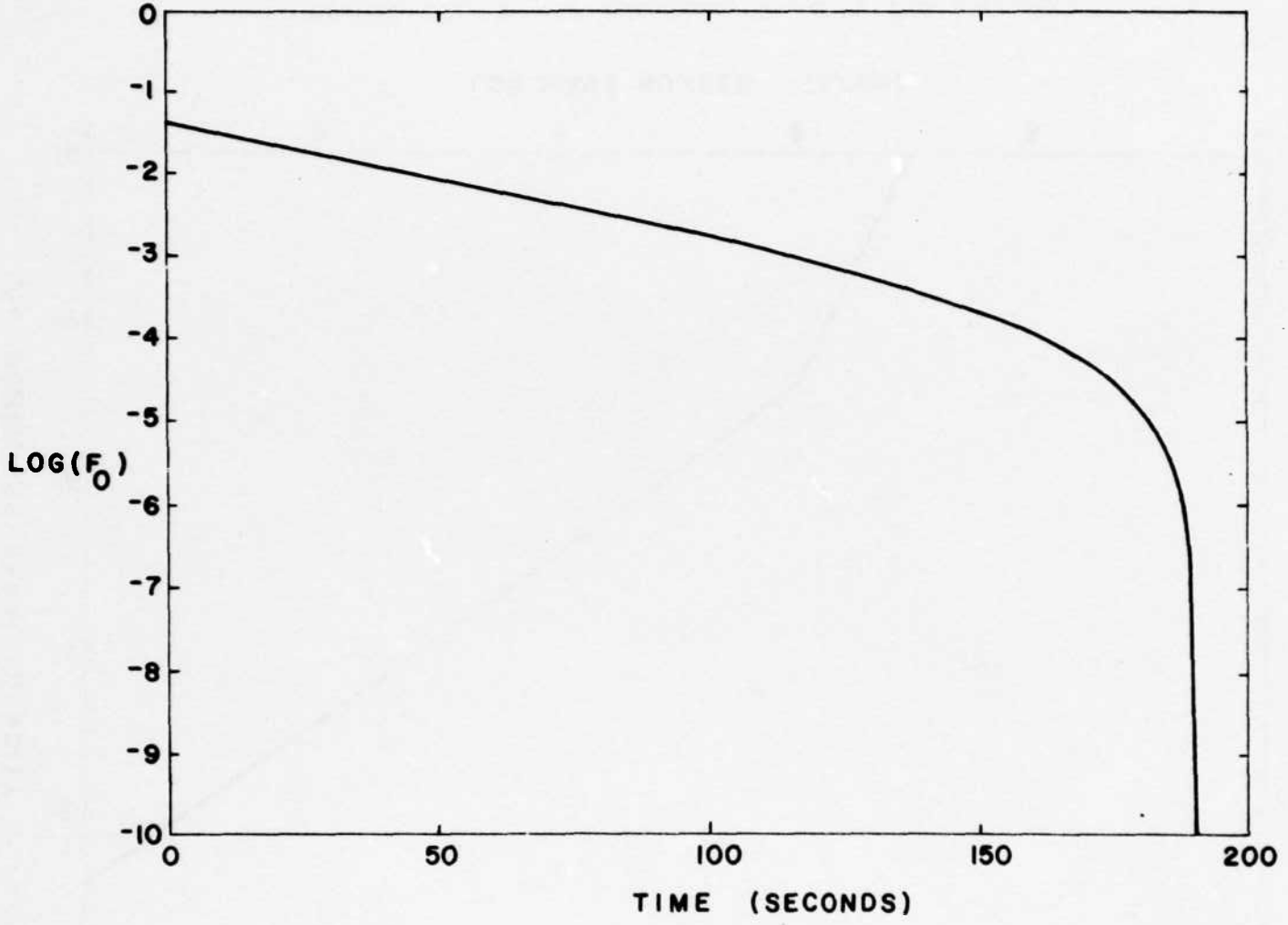

Figure 8E. Power summation in the macroscale versus time, case 5.

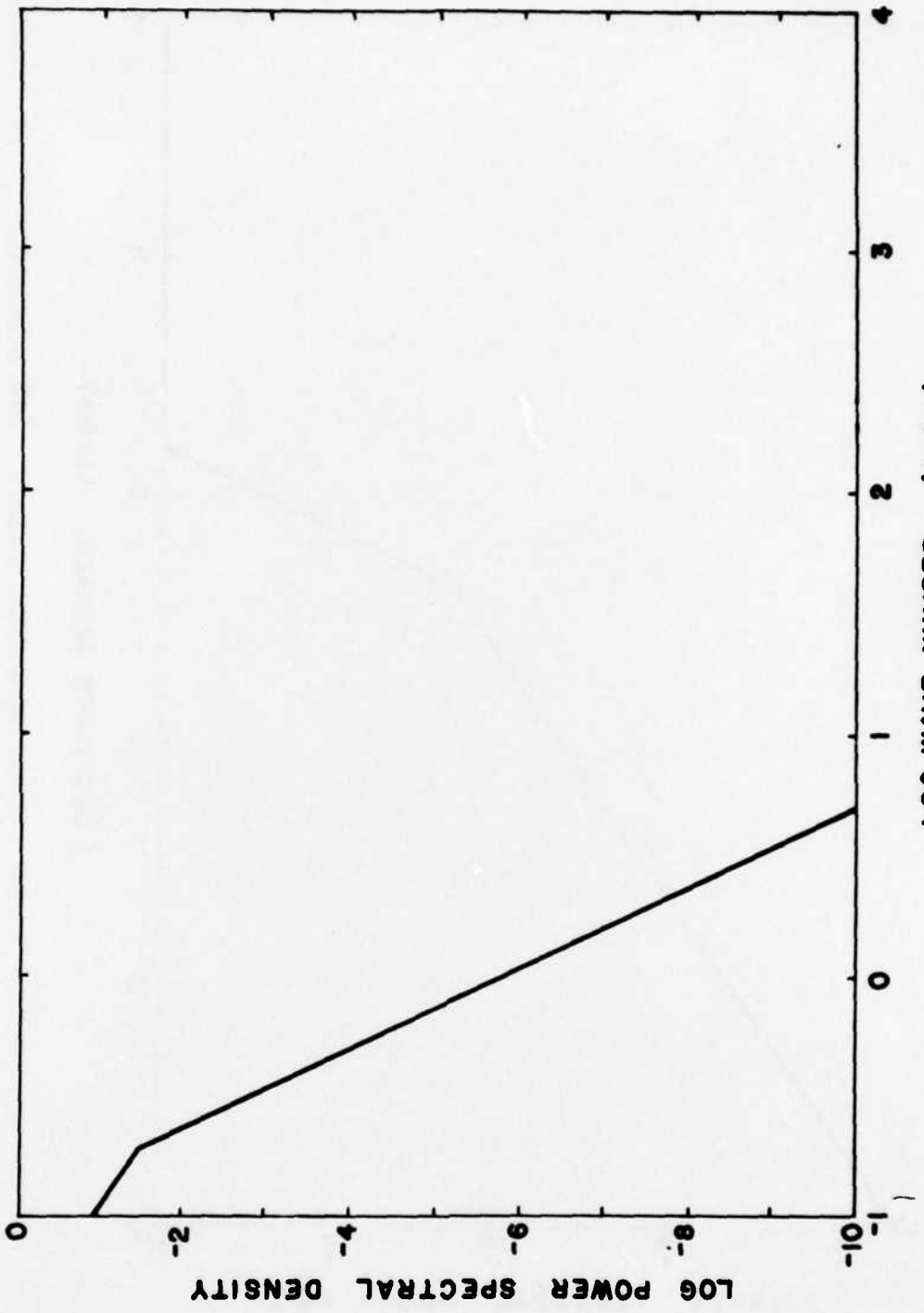

Figure 8F. Power spectrum, case 5, 200 seconds.

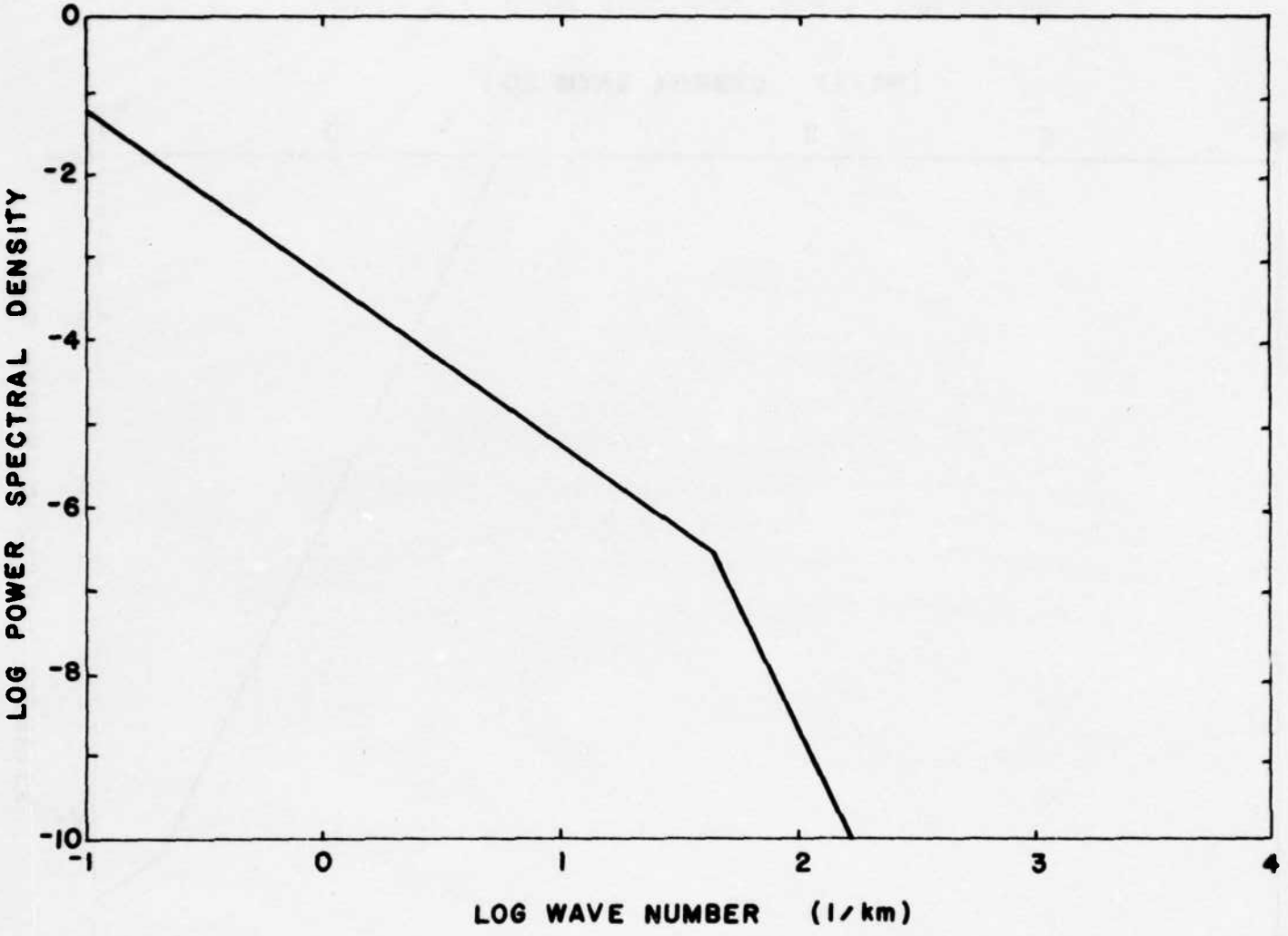

Figure 8G. Power spectrum, case 5, 250 seconds.

microstructure regime is feeding totally on itself and is in a state of continuing decay.

By 300 seconds, in Figure 8H, the basic cascade pattern is completely re-established. This pattern will persist to the very end. Figure 8I shows the spectrum at 1800 seconds, while Figure 8J displays the scenario at 17,000 seconds. Left to run indefinitely, the program will push the cascade "into the mud" asymptotically.

Case 5 is, perhaps, the best demonstration of the power of the model to compute late-time behavior of microstructure.

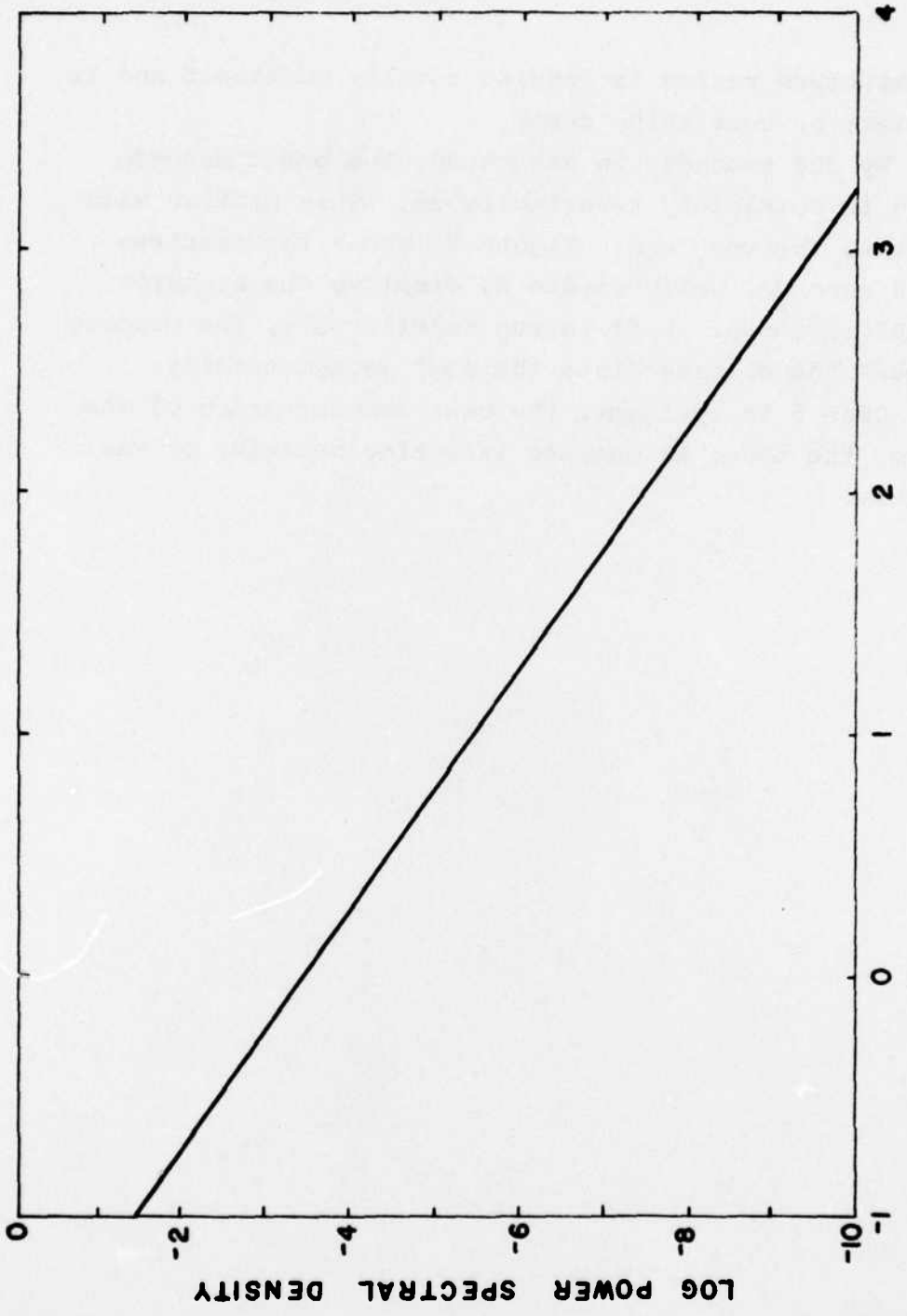

Figure 8H. Power spectrum, case 5, 300 seconds.

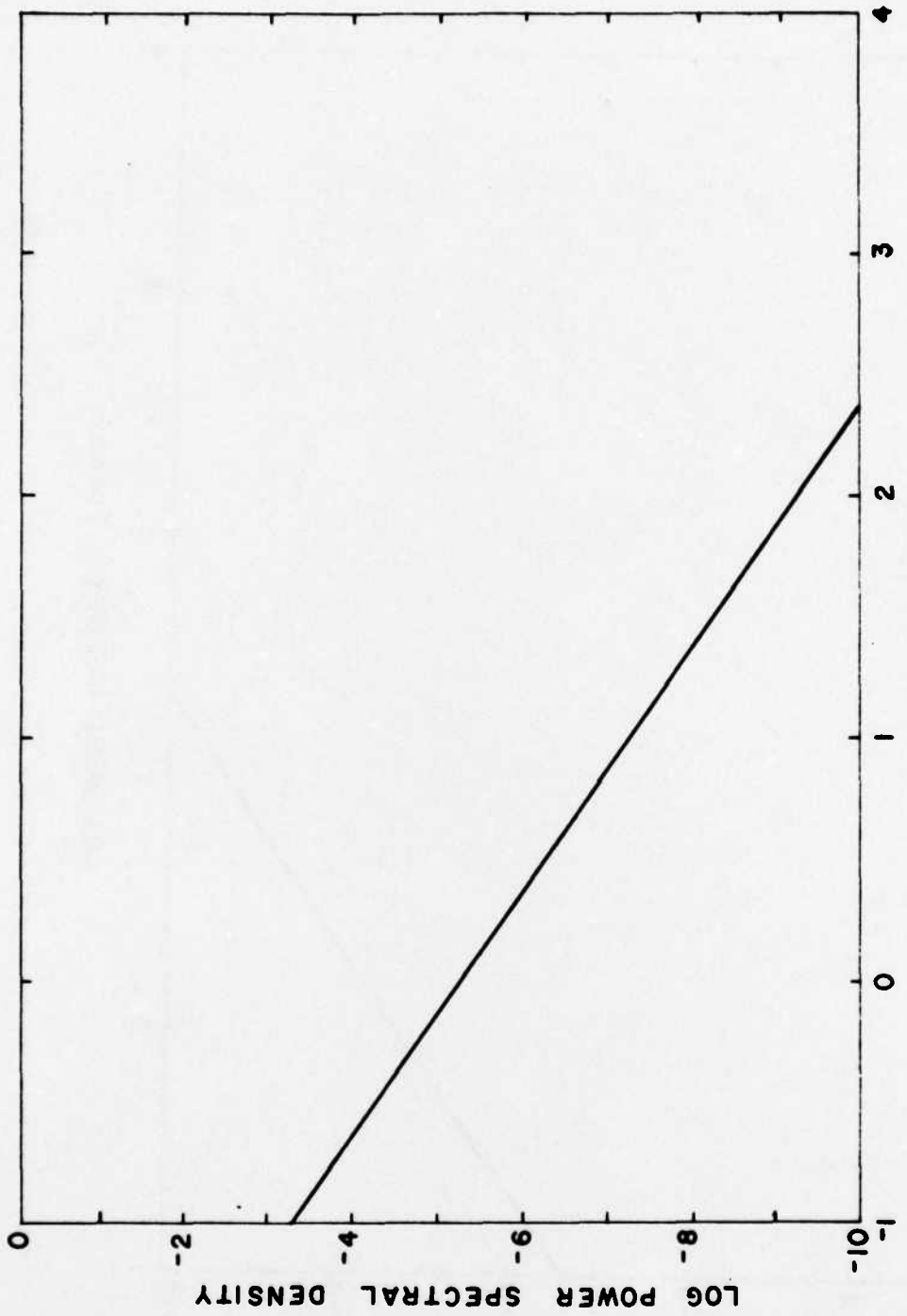

Figure 61. Power spectrum, case 5, 1800 seconds.

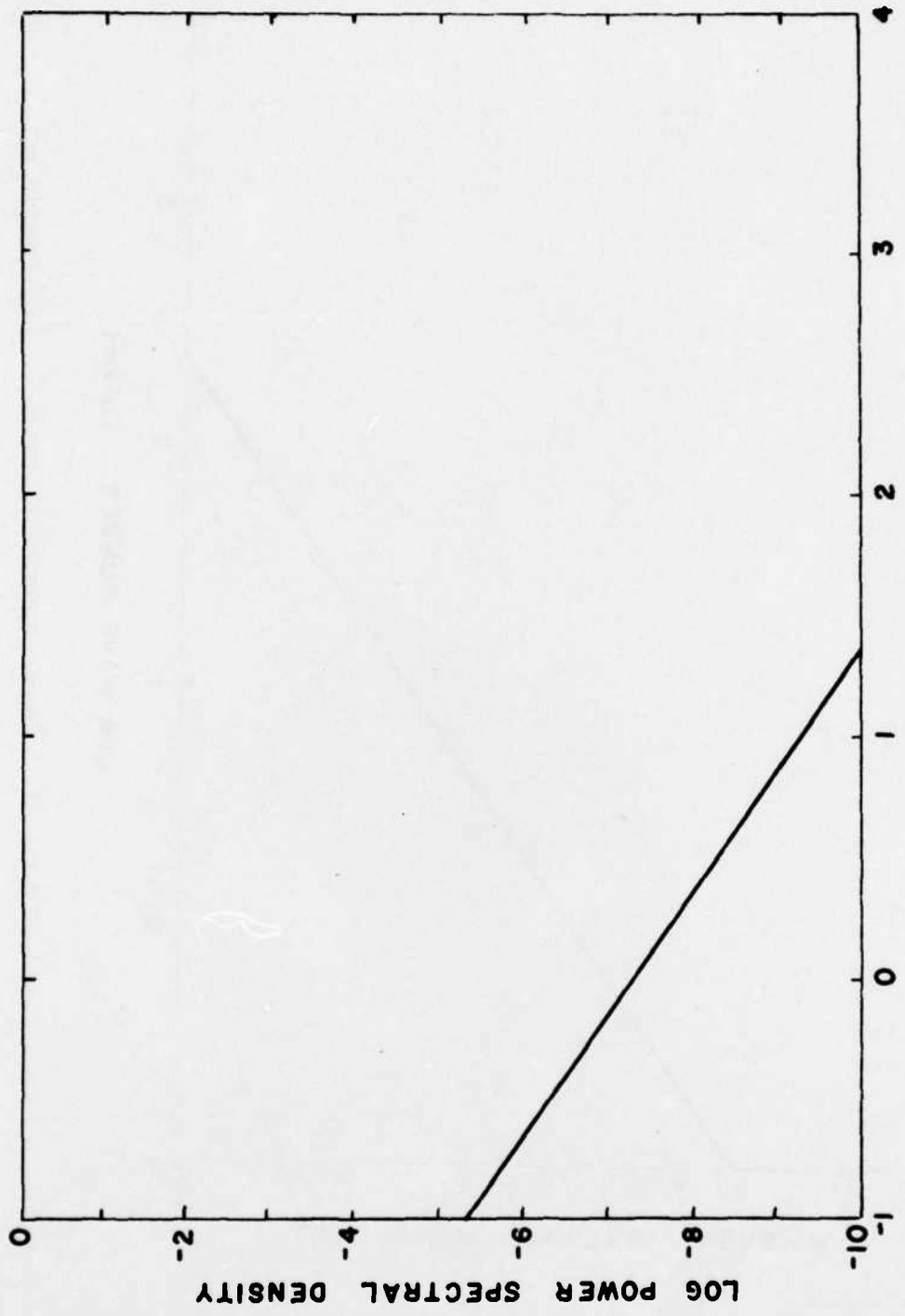

Figure 8J. Power spectrum, case 5, 17,000 seconds.

V. CONCLUSION AND APPLICATION

The gradient drift microstructure model that has been developed is capable of spanning many orders of magnitude in scale size and includes the important physics of cascade and ultimate diffusion. It is believed to contain all of the best, current thinking on gradient drift theory but, of necessity, remains an approximation to the solution of the basic plasma conservation equations.

Adjustable coefficients have been provided to tune the actual numerical results so as to provide close agreement with both the current experimental data base and the numerical results of computer simulation of microstructure.

While the rate expressions and associated constitutive relations may appear complicated, they are in essence only a simple one-dimensional set. For simple exploratory work, a BASIC program which runs on the tabletop Tektronix 4051 is usually employed. For use in actual systems analysis, an extremely fast program for the CDC 7600 has been built. In actual application, the microstructure program is only one routine in a larger matrix of programs employed to analyze UHF communication in the nuclear environment. The detailed description of the actual application and associated numerics will be the subject of future reporting.

VI. BIBLIOGRAPHY

The most important documents which provide the history, background, and application of gradient drift physics and associated plasma microstructure modelling are in the classified literature. Reviewing, referencing, and discussing these materials would have caused the present document to be classified itself. As our current work represents a completely new approach to the problem and does not rely, from a technical standpoint, on this older material, we have felt justified in avoiding a formal set of references. As a general bibliography, for readers who are unfamiliar with the field, we will indicate three papers in the open literature which provide useful background.

A. For the application of gradient drift physics to the study of barium clouds and a review of basic theory, we recommend: Linson, L.M., and J.B. Workman, "Formation of Striations in Ionospheric Plasma Clouds", J. Geophys. Res., 75, 3211 (1970).

B. For the theoretical study of the basic gradient drift equations, mode coupling, and cascade, we recommend: Rognlien, T.D., and J. Weinstock, "Theory of the Nonlinear Spectrum of the Gradient Drift Instability in the Equatorial Electrojet", J. Geophys. Res., 79, 4733 (1974).

C. For an example of the current state of the art in numerical simulation of gradient drift microstructure, we recommend: McDonald, B.E., S.L. Ossakow, S.T. Zalesak and N.J. Zabusky, "Determination of Minimum Scale Sizes in Plasma Cloud Striations", Proceedings of the 1978 Ionospheric Effects Symposium, January 1978, published by Naval Research Laboratory.

DISTRIBUTION LIST

DEPARTMENT OF DEFENSE

Assistant to the Secretary of Defense
Atomic Energy
ATTN: ATSD (AE)

Director
Command, Control Technical Center
ATTN: C-650

Director
Defense Advanced Rsch. Proj. Agency
ATTN: Nuclear Monitoring Research
ATTN: Strategic Tech. Office

Director
Defense Communications Agency
ATTN: Code 101B

Defense Documentation Center
Cameron Station
12 cy ATTN: TC

Director
Defense Nuclear Agency
ATTN: DDST
ATTN: TISI
3 cy ATTN: TITL
ATTN: RAAE
ATTN: STVL

Commander
Field Command
Defense Nuclear Agency
ATTN: FCPR

Chief
Livermore Division, Fld. Command, DNA
Lawrence Livermore Laboratory
ATTN: FCPRL

Under Secretary of Def. for Rsch. & Engrg.
ATTN: S&SS (OS)

DEPARTMENT OF THE ARMY

Commander
Harry Diamond Laboratories
ATTN: DELHD-TI
ATTN: DELHD-NP
ATTN: DELHD-NP, F. Wimenitz

Commander
U.S. Army SATCOM Agency
ATTN: Document Control

Commander
U.S. Army Nuclear & Chemical Agency
ATTN: Library

DEPARTMENT OF THE NAVY

Chief of Naval Operations
ATTN: OP 943, LCDR Huff

Chief of Naval Research
ATTN: Code 461

DEPARTMENT OF THE NAVY (Continued)

Commanding Officer
Naval Intelligence Support Ctr.
ATTN: STIC 12, Mr. Dubbin

Commander
Naval Ocean Systems Center
ATTN: Code 2200

Director
Naval Research Laboratory
ATTN: Code 7700, S. Ojjakow

Officer-in-Charge
Naval Surface Weapons Center
ATTN: Code WA501, Navy Nuc. Prgms. Off.

DEPARTMENT OF THE AIR FORCE

AF Geophysics Laboratory, AFSC
ATTN: PHD, J. Mullen
ATTN: SUOL
ATTN: PHP, J. Aarons

AF Weapons Laboratory, AFSC
ATTN: DYT
ATTN: SUL

AFTAC
ATTN: TN

Air Force Avionics Laboratory, AFSC
ATTN: AAD, A. Johnson

Commander
Foreign Technology Division, AFSC
ATTN: NICD, Library

Commander
Rome Air Development Center, AFSC
ATTN: EMTLD

DEPARTMENT OF ENERGY

University of California
Lawrence Livermore Laboratory
ATTN: Doc. Con. for Tech. Info. Dept.

Sandia Laboratories
ATTN: Doc. Con. for W. Brown

DEPARTMENT OF DEFENSE CONTRACTORS

Aerospace Corp.
ATTN: D. Olsen

Charles Stark Draper Laboratory, Inc.
ATTN: D. Cox

ESL, Inc.
ATTN: J. Marshall
ATTN: C. Prettie

General Electric Company-TEMPO
Center for Advanced Studies
ATTN: DASIAC

DEPARTMENT OF DEFENSE CONTRACTORS (Continued)

General Research Corp.
Santa Barbara Division
ATTN: J. Ise, Jr.

JAYCOR
ATTN: S. Goldman

McDonnell Douglas Corp.
ATTN: Tech. Library Services

Mission Research Corp.
ATTN: R. Kilb
ATTN: R. Bogusch
ATTN: R. Hendrick

Mitre Corp.
ATTN: W. Sen

R & D Associates
ATTN: R. Lelevier
ATTN: B. Gabbard

DEPARTMENT OF DEFENSE CONTRACTORS (Continued)

Physical Dynamics Inc.
ATTN: F. Chu
ATTN: J. Workman

Rand Corp.
ATTN: C. Crain
ATTN: F. Bedrozian

Science Applications, Inc.
ATTN: D. Sachs

SRI International
ATTN: W. Chestnut
ATTN: C. Rino
ATTN: D. McDaniel